Reactive Oxygen Species (ROS) up-regulates MMP-9 expression via MAPK-AP1 signaling pathway in rat astrocytes.

The thesis presented to
The Faculty of Graduate and Post-Doctoral Studies
Of
University of Ottawa

By Elizabeth Malcomson

In partial fulfillment of the requirements for
Master Degree of Science in Neuroscience
NSC Graduate Program
University of Ottawa

February 2011

Thesis Advisor
Dr. Wandong Zhang

Abstract

Ischemic stroke is characterized by a disruption of blood supply to a part of the brain tissue, which leads to a focal ischemic infarct. The expression and activity of MMP-9 is increased in ischemic stroke and is considered to be one of the main factors responsible for damages to the cerebral vasculature, resulting in compromised blood-brain barrier (BBB) integrity. However, the regulatory mechanisms of MMP-9 expression and activity are not well established in ischemic stroke. Since hypoxia/ischemia and reperfusion generates reactive oxygen species (ROS), I hypothesize that ROS is one of factors involved in up-regulation of MMP-9 expression in brain cells and ROS-mediated effect may occur via MAPK signaling pathway. My study has provided the evidence that ROS is responsible for an increase in MMP-9 expression in astrocytes mediated via MAPK-AP1 signaling pathway. Preliminary studies with an *in vitro* model of the BBB suggest that inhibition of MMP-9 is a critical component of reducing ROS-induced BBB permeability.

Table of Contents

LIST OF FIGURES

List of Tables

List of Abbreviations

AJ	adherens junctions
AP-1	activator protein 1
BBB	blood-brain barrier
CNS	central nervous system
DMEM	Dulbecco's modified Eagle's medium
DNA	deoxyribonucleic acid
ERK	extracellular signal-regulated kinases
FBS	fetal bovine serum
HEK	human embryonic kidney
H_2O_2	hydrogen peroxide
JNK	c-Jun N-terminal kinases
LHP	linoleic acid hydroperoxide
MAPK	mitogen-activated protein kinase
MCP-1	monocyte chemotactic protein-1
MCAO	middle cerebral artery occlusion
MMP	matrix metalloproteinase
NRA	neonatal rat astrocytes
NVU	neurovascular unit
oxLDL	oxidized low-density lipoprotein
PCR	polymerase chain reaction
ROS	reactive oxygen species
SOD1	superoxide dismutase

TJ	tight junctions
TIMP	tissue inhibitors of metalloproteinases
tPA	tissue plasminogen activator
TPA	12-O-tetradecanoyl phorbol-mycetate-acetate
VEGF	vascular endothlial growth factor
ZO-1	zona occludens- 1

Acknowledgements

First and foremost I would like to thank my supervisor Dr. Wandong Zhang for the opportunity to train in his laboratory and pursue graduate studies. I would also like to thank Drs Danica Stanimirovic, Quing Liu and Stephanie Bennet for being on my advisory committee and providing feedback and guidance for my project. To Debbie Callaghan, to whom a million thank you's would never suffice, I want you to know how grateful I am for all the training and support. A big hug to Shanshan Shen, thank you Shan^2 for always offering a helping hand and believing in me, I will miss you dearly but we will be lifelong friends! In addition I would like to thank all members of the Zhang lab, especially Huaqi Xiong for his experimental expertise and Camille Juzwik for all the laughs, and Joy Lei in Dr. Q. Liu's lab for her help on TIMP1 project. I would also like to thank all of the people I had the privilege of meeting and working with at the Institute for Biological Sciences at the National Research Council of Canada. To Ashley and Erin: thank you for all the laughs, love and support. Trevor, you helped me keep the challenging days in perspective and were my best friend through this process. To my big brother Allan, you have and always will be my rock and dearest friend. Lastly I would like to thank my parents for their unwavering support, puppy sitting and home-cooked meals. Dad, thank you for teaching me the meaning of hard work and cultivating my love for learning. To my Mom, thank you for not only allowing me the chance to pursue all of my dreams but believing in every single one of them.

This study was supported by a research grant from the Heart and Stroke Foundation of Ontario (HSFO) to Dr. W. Zhang.

Chapter 1: Introduction

Cerebral ischemia and reperfusion are two pathological conditions that lead to oxidative stress and blood-brain barrier (BBB) breakdown. Current research suggests that matrix metalloproteinase 9 (MMP-9) can be activated by reactive oxygen species (ROS) produced during ischemia and reperfusion and that ROS-induced up-regulation of MMP-9 is one of the main factors responsible for degrading the extracellular matrix (ECM) proteins of cerebral vascular basal membrane and the tight junctions between cerebral endothelial cells leading to disruption of BBB integrity. Disruption of BBB integrity has dire consequences on the central nervous system (CNS), resulting in brain edema, infiltration of inflammatory cells, secondary brain damage and poor neurological outcomes (Rosell *et al.* 2006; Zlokovic 2006). The objective of this research is to examine the molecular signaling mechanisms by which MMP-9 becomes up-regulated by ROS-induced oxidative stress in ischemic stroke by using *in vitro* models whereby interference with this pathway could be developed as an approach to reduce MMP-9- mediated BBB breakdown.

1.1 Cerebral ischemia and the blood-brain barrier

Stroke is defined as an interruption in blood flow to a part of brain tissue which depending on severity and location can disrupt brain function. The interruption in blood flow can be due to a blockage of a cerebral artery namely an ischemic stroke (Figure 1. a) or rupture of blood vessels in the brain namely a hemorrhagic stroke (Figure 1. b). Interruption of blood flow results in a lack of oxygen and nutrient delivery to part of the brain which damages the tissues. Ischemic stroke or cerebral ischemia is responsible for 80% of all stroke patients which taken in combination is the number one cause of disability and third leading cause of

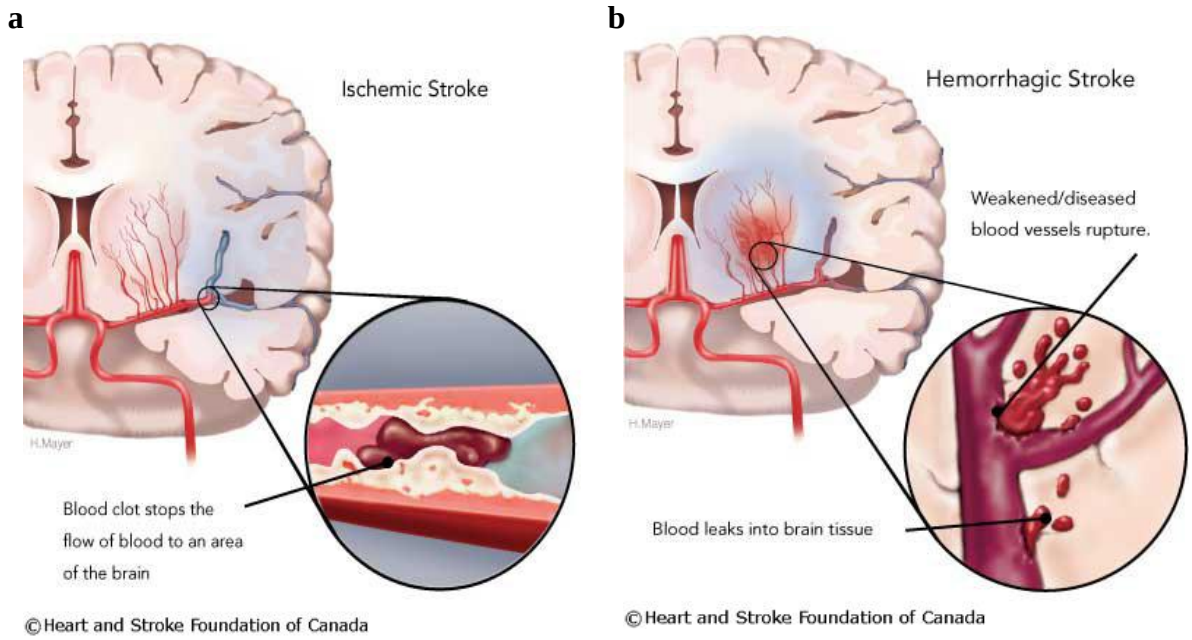

Figure 1. Schematic of two main types of stroke

A stroke is characterized by a sudden loss of brain function caused by a reduction of blood supply to the brain tissue. The type of stroke is defined by the cause of the reduction in bloody supply. When a thrombus or an embolus causes a blockage in a cerebral artery, preventing blood flow to brain tissue, this is called an ischemic stroke (a). When a blood vessel ruptures resulting in uncontrolled bleeding in the cerebral tissue, this is called a hemorrhagic stroke (b). Stroke is the third leading cause of death in Canada, whereby 6% of the population will die due to stroke. Of these strokes, 80% are ischemic stroke and 20% are hemorrhagic. Statistics and images were obtained from the Heart and Stroke Foundation of Canada.

death amongst Canadians (Heart and Stroke Foundation of Canada 2010). This statistic highlights the importance of stroke research. At the present time, the only pharmacological treatment for ischemic stroke is tissue plasminogen activator (tPA) therapy. Tissue plasminogen activator (tPA) is a serine protease that cleaves the precursor molecule plasminogen to generate plasmin. Plasmin, the active enzyme, dissolves fibrin-based clots typical of ischemic stroke. tPA therapy has several caveats including a narrow window for administration of three hours of stroke on-set and its association with hemorrhagic transformations, edema, neurotoxic effects and BBB injury (Lee *et al.* 2007; Pfefferkorn and Rosenberg 2003). Thus, further stroke research is important to provide insight into the factors and signaling pathways responsible for BBB disruption in ischemic stroke and new types of therapeutic intervention for patients to minimize brain damage and to promote recovery.

The BBB functions in the neurovascular unit (NVU) to provide both a physical and biological barrier between circulating peripheral blood flow and CNS (Wolburg and Lippoldt 2002; Zhang and Stanimirovic 2005). By providing this barrier, the BBB maintains the CNS homeostasis, which is required in order to have "proper functioning of neuronal circuits, synaptic transmission, synaptic remodeling, angiogenesis and neurogenesis in the adult brain" (Zlokovic 2008). For the purpose of my research it is important to understand the function and structure of the BBB. The BBB is a highly specialized structure of cerebral endothelial cells that together with pericytes, astrocyte end-foot processes, microglia and the extracellular matrix make up the neurovascular unit (NVU) (Figure 2). The BBB is

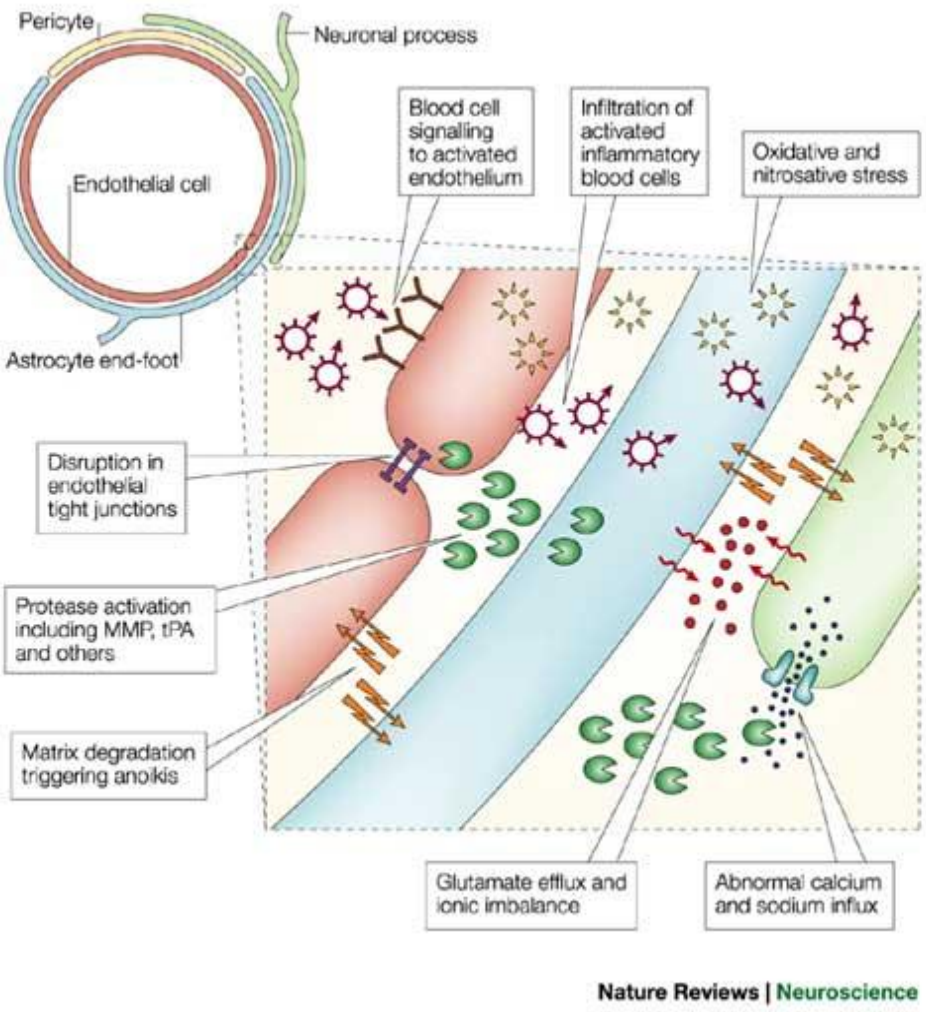

Figure 2. Schematic representation of the neurovascular unit (NVU).

The neurovascular unit (NVU) is comprised of endothelial cells, astrocytes, extracellular matrix, basal lamina, adjacent neurons and pericytes. Together they provide functional integrity to the blood-brain-barrier (BBB) and maintain normal cell signaling through homeostasis. Cerebral ischemia results in loss of integrity in the NVU and initiates signaling cascades of cell injury. For example, in this schematic oxidative stress upregulates matrix metalloproteinases (MMPs), which cause BBB leakage, and this leakage allows for infiltration of inflammatory cells resulting in greater damage to the brain tissue.

described as a composition of tightly sealed brain endothelial cells connected by transmembrane proteins occludins and claudins which form tight junctions (TJ) and adheren junctions (AJ) (Hawkins and Davis 2005). The high density of TJ and AJ between the BBB cells results in a low paracellular permeability and high electrical resistance (Romero *et al*. 2003). The endothelial cells that make up the BBB are described by Hawkins and Davis (2005) as having a number of anatomical characteristics that make them differentiable from peripheral endothelial cells: including an increased number of mitochondria (Oldendorf et al. 1977), lack of fenestrations (Fenstermacher et al. 1988), and high-density TJ (Kniesel and Wolburg 2000). Perictyes, a connective tissue type cell, are attached at irregular intervals to the albumnial membrane of the endothelium (Tagami et al. 1990) that along with endothelial cells are wrapped in basal lamina sheath (Farkas and Luiten 2001). This basal lamina membrane, made up of collagen type IV, heparin sulfate proteoglycans, laminin, fibronectin, and other ECM proteins, is attached to the plasma membranes of astrocytic end-feet (Hawkins and Davis 2005).

Similar to the structural physiology the molecular physiology of the BBB is unique and critically important for providing a physiological barrier allowing the passage of beneficial molecules and preventing passage of harmful molecules. The transport of molecules across the BBB is tightly regulated by many different transport systems: carrier mediated transporters and active efflux transporters (Zhang and Stanimirovic 2005; Zlokovic 2008). In addition, endothelial cells of the BBB provide a metabolic barrier by expressing enzymes capable of modifying endogenous and exogenous molecules that may pass the physical barrier and have a negative effect on neuronal function (Pardridge 2005). Due to the dual role the BBB plays in maintaining the neurovascular unit and protecting neuronal tissue,

BBB breakdown in cerebral ischemia is a key component in the pathophysiology of ischemic stroke.

1.2 Matrix metalloproteinase-9 mediated blood-brain barrier breakdown

MMP-9 belongs to the family of matrix metalloproteinases (MMPs) which are known for their "dependence on metal ions for catalytic activity and their potent ability to degrade structural proteins of the extracellular matrix" (Stocker and Bode 1995). The MMPs are a family of functionally and structurally homologous proteins. They exist as secreted or membrane-bound enzymes that require activation through proteolytic processing from their pro-form (zymogen) to their active form (Cunningham et al. 2005). MMPs are divided into four families based on their structure and substrate specificity: collagenases, gelatinases, stromelysins, and membrane associated MMPs. The MMP family plays a role in physiological processes such as embryogenesis, tissue remodeling, wound healing, and angiogenesis as well as in disease states such as inflammatory disease, metastasis in cancer, and arthritis (Sternlicht and Werb 2001). Recently, scientific research has recognized a role for MMPs in cortical changes of the brain following cerebral ischemia. In particular, MMP-9, the most widely studied of the metalloproteinase family, has been identified as being the most responsive MMP to acute brain injury (Lee *et al.* 2006).

MMP-9 together with MMP-2 make up the MMP gelatinase family, as they are both capable of degrading type IV collagen, the major constituent of basement membranes of cerebral vessels. Although these two MMPs share structural and catalytic similarities, they have independent transcription due to different regulatory elements within their promoters (Hong *et al.* 2005). Structurally, MMP-9 is composed of a signal peptide domain, a pro-domain, a

catalytic domain, a hemopexin-like domain, a hinge region, a fibronectin-like gelatin binding domain, and a collagen-liked domain. The pro-domain is critical for maintaining the latency of MMP-9. Once the pro domain is removed by proteolysis the enzyme is activated. The process of activation is called the "cysteine switch" whereby a conformational change occurs making the catalytic zinc accessible for a hydrolytic water molecule and for the substrate (Ram *et al.* 2006). In addition to autoactivation, there are several activators of latent MMP-9 including leukocytes, proteases and ROS (Rajagopalan *et al.* 1996). MMP-9 is expressed in the healthy adult brain at relatively low levels (Cunningham et al. 2005). However, MMP-9 up-regulation occurs in neurons, astrocytes, oligodendrocytes, microglia and endothelial cells following acute brain injury. This level of MMP-9 expression differs by the type (focal vs. global ischemia) (Rosenberg and Mun-Bryce 2004) as well as by the duration and severity of the insult (Cunningham *et al*. 2005). The up-regulation of MMP-9 plays a deleterious role in the processes of extracellular proteolysis which contributes to tissue damage following acute brain injury (Asahi *et al.* 2001), with the major pathological effect of MMP-9 activity being the opening of the BBB compromising its integrity (Cunningham *et al*. 2005). Compromised BBB integrity means the biological and physical barrier is no longer able to maintain the homeostasis of the central nervous system (CNS) (Wolburg and Lippoldt 2002).

An important aspect of this finding is to understand the mechanism by which MMP-9 is capable of opening the BBB and disrupting its integrity. As previously mentioned, the physical barrier is made up of tight junctions between endothelial cells that restrict the passage of solutes between the blood and brain. These tight junctions are built upon the

endothelial cell matrix made up of collagens, laminin and fibronectin. Collagen type IV has been shown to directly influence the expression of occludin, an integral plasma-membrane protein located specifically at tight junctions (Savettieri *et al.* 2000). Loss of laminin, collagen and fibronectin can disrupt the endothelial tight junctions and loss of BBB integrity (Hamann *et al.* 1995). How MMP-9 disturbs BBB integrity, is by specifically attacking these components of extracellular matrix, which has been demonstrated by several studies. The idea that degradation of the extracellular matrix protein and disruption of basal lamina is the primary cause of microvascular hemorrhage following an ischemic event has led to the report of a close relationship between BBB leakage and MMP-9 expression in animal models of cerebral ischemia (Fujimura *et al.* 1999). Elevated MMP-9 levels have been shown to coincide with a direct neurological outcome, suggesting that MMP-9 plays a role in neuronal death and brain injury following ischemic stroke (Montaner *et al.* 2005). MMP-9 knockout study has demonstrated that the MMP-9 deficient mice are protected against brain trauma and focal cerebral ischemia (Wang *et al.* 2000) and show reduced BBB leakage (Asahi *et al.* 2001). MMP-9 inhibitors have been shown to prevent laminin degradation, which maintains the extracellular matrix and BBB integrity and protects neurons from apoptosis (Gu *et al.* 2005; Romanic *et al.* 1998). Thus, increased levels of MMP-9 following acute brain ischemic injury have been linked to greater infarct size, poor neurological outcome, and hemorrhagic transformation complications (Rosell and Lo 2008). MMP-9 is currently being explored as a potential pharmacological target and biomarker of stroke, as high levels of this protease is detected in the blood of human patients following ischemic and hemorrhagic strokes in comparison to healthy individuals (Montaner *et al.* 2001).

The aforementioned research implicates a pathophysiologic role for MMP-9 in the disruption of the BBB permeability following cerebral ischemia and reperfusion and that inhibition of MMP-9 expression may have a neuroprotective action following cerebral ischemia. However the molecular mechanisms responsible for MMP-9 up-regulation in ischemic stroke have yet to be fully elucidated. Therefore, as previously mentioned the goals of this research are to provide the insight and characterize the specific mechanisms that regulate MMP-9 expression in ischemic stroke.

1.3 Potential Mechanisms of MMP-9 activation: MCP-1, VEGF and ROS

1.3.1 Role of MCP-1 and VEGF on MMP-9 Expression

MMPs may be regulated at the level of transcription via chemokines, cytokines and growth factors released during cerebral ischemia and neuroinflammation. Monocyte chemoattractant protein 1 (MCP-1) and Vascular Endothelial Growth Factor (VEGF) are two factors that have been identified as being up-regulated following ischemic brain damage and have potential as regulatory mediators of MMP-9 expression (Cross and Woodroffe 1999; Valable 2005; Lee *et al.* 2007; Mojsilovic-Petrovic *et al.* 2007; Ahmad *et al.* 2009; Narasismhan *et al.* 2009). MCP-1, a potent chemokine, along with other chemokines directs blood-borne monocytes/macrophages across the BBB into inflammatory sites in the brain. Proinflammatory chemokines play a role following ischemic damage in neuroinflammation by which monocytes/macrophages remove dead cells and inflammatory mediators stimulate multipotent cells to differentiate to functional neuronal or glial cells in the injured area (Zhang and Stanimirovic 2002). Both the *in vitro* and *in vivo* findings suggest that

hypoxia/ischemia-induced infiltration of monocytes and macrophages contributes to the pathophysiology and damage induced by stroke as well as MMP-9 upregulation. MCP-1 *in vitro* work has shown an upregulation in fetal human astrocytes following hypoxia and cobalt chloride treatment linked to neuroinflammation (Mojsilovic-Petrovic *et al.* 2007). In addition, one study found that treatment of a human fetal microglial cell line CHME3 with MCP-1, MIP1β, RANTES, IL-8, and Fractalkine for 24 h increased the secretion of MMPs and TIMPs. MCP-1, MIP1β, and Fractalkine also increased MMP-9 secretion in primary rat brain microglia *in vitro* (Cross and Woodroofe 1999), but the molecular mechanism of transcriptional regulation was not characterized in this study. Furthermore, the evidence provided by *in vivo* work demonstrated that infiltrating blood-borne monocytes and macrophages attracted by MCP-1 were recruited into ischemic tissue as early as 18 h following transient middle cerebral artery occlusion (MCAO) in mice (Weiss *et al.* 1998; Chen *et al.* 2003). Astrocytes, part of the proposed *in vitro* model, are the main cytokine and chemokine producing cells in the brain (Andejelkovic *et al.* 2000) and therefore are a good model to determine if MCP-1 is involved in MMP-9 upregulation following cerebral ischemia and reperfusion.

The interaction between VEGF and MMP-9 demonstrates another deleterious effect of cerebral ischemia. The VEGF family and its receptors are important signaling proteins involved in the development, maintenance and remodeling of the vasculature through two main process: vasculogenesis and angiogenesis (Gabhann and Popel 2008). VEGF exists in 7 isoforms from VEGF-A to VEGF-F, which vary in amino acid resides from 165-206.

VEGF-A is the most important isoform in the developing CNS, as well as, the most potent inducer of BBB breakdown (Argaw *et al.* 2008).

Previous research shows that VEGF and MMP-9 are involved in increasing the permeability of the endothelium, which leads to vasogenic edema (Bates *et al.* 2002). One study using oxygen deprivation has shown that VEGF becomes one of the most potent soluble factors, and causes a hyper-permeability of endothelial cells (Ahmad *et al.* 2008). VEGF *in vivo* research on a rat stroke model (MCAO) revealed that two rat VEGF isoforms are present in the ischemic cortices 3 hours after occlusion (Valable *et al.* 2005). The aforementioned work was paired with exogenous treatments, which revealed administration of VEGF exacerbated BBB leakage during cerebral ischemia whereas a late administration of VEGF promotes angiogenesis. Furthermore, the effects of exogenous VEGF were compared to the kinetic activity of MMP-9, which revealed MMP-9 expression that paralleled the kinetics of the BBB opening in response to cerebral ischemia (Valable *et al.* 2005). The research suggests that VEGF could be playing a regulatory role in MMP-9 expression and activity.

1.3.2 ROS-induced Oxidative Stress, MMP-9 Expression and BBB breakdown

Oxidative stress is a major factor to consider in this research as it has been shown to regulate the proteins comprising junctions of the BBB where reactive oxygen species (ROS) plays a significant role in BBB disruption and brain edema. Previous studies in cell culture and animal models have indicated a free-radical induced oxidative stress as playing a significant role in ischemic brain injury (Kondo *et al*. 1997; Gasche *et al.* 2001; Kamada *et al*. 2007). More specifically, oxidative stress in cerebral ischemia and reperfusion can play a profound

role in the disruption of the BBB (Shukla 1993). ROS are present in many forms such as superoxide, hydroxyl radicals, hydrogen peroxide, singlet oxygen and in the case of my research H_2O_2 (hydrogen peroxide). For the purpose of my study, it is important to note the relationship between oxidative stress and MMP-9 expression/activation. Recent works have shown that inhibition of MMP can prevent this oxidative stress-induced BBB disruption in ischemia (Kondo 1997; Gashe 2001). The mechanism of action for ROS-mediated MMP activation was demonstrated *in vitro* by Rajagoplan (1996), which showed ROS can oxidize a thiol bond responsible for activating MMP-2 and MMP-9. This suggests that macrophages activated during ischemia and reperfusion that release ROS can trigger the activation of stored latent forms of MMP-9 in the vascular regions of the BBB. This was illustrated by a loss of function study on mice lacking copper/zinc-superoxide dismutase (SOD1). These mice are highly susceptible to focal cerebral ischemia-reperfusion with exacerbated vasogenic edema and a higher mortality than wild-type animals (Kondo *et al.* 1997). Furthermore, recent studies using mice deficient in SOD1, have shown that inhibition of MMPs resulted in a reduction of the ischemia/reperfusion-induced BBB disruption. In addition, research performed by Ashai and colleagues (2000) showed that the inhibitor of ROS prevented tPA–triggered cerebral hemorrhage after stroke. In human patients oxidative stress has been shown to contribute to the pathogenesis of several neurodegenerative diseases and cerebravascular disorders such as stroke and Alzheimer's disease (Uno et *al*. 2005). A recent human study evaluating biomarkers of antioxidant therapies in stroke (BEAT-Stroke) shows that there is an increase in oxidative stress and this is related to MMP-9 expression (Kelly *et al.* 2009). The aforementioned findings suggest

that latent form MMP-9 is activated at the protein level by oxidative stress and together these factors mediates BBB breakdown.

1.4 TIMP1 and MMP-9

MMPs may be regulated at the level of transcription via chemokines, cytokines, and growth factors released during ischemic stroke and neuroinflammation. MMPs are regulated at the protein level by endogenous activators and inhibitors that affect the factors such as secretion, cell surface localization, degradation and removal (Sternlicht and Werb 2001). MMPs are synthesized as inactive zymogens that require proteolytic activation (Harper *et al*. 1971). There are now at least four known endogenous metalloproteinase inhibitors, called tissue inhibitors of metalloproteinases (TIMPs) that inhibit MMPs' activities (Sternlicht and Werb 2001). TIMPs are dimers consisting of an N-terminal domain, and a smaller C-terminal domain, where the N-terminal domain, non-covalently binds to the MMP substrate at the active binding site for MMP inhibition (Gomez *et al.* 1997; Nagase *et al.* 1999). TIMPs act in two ways, either by inhibition of the catalytically active form of the enzyme as previous described or through prevention of the conversion of matrix metalloproteinase from zymogens to the active form (Bodden *et al*. 1994). An imbalanced ratio between MMP/TIMP may have implications in the pathophysiology of CNS diseases and inflammation. Expression of the four TIMPS (TIMP-1, TIMP-2, TIMP-3, and TIMP-4) varies spatial and temporally throughout the nervous system. Of the most interest is TIMP-1, which inhibits MMP-9 activity (Fager and Jaworski 2000; Vaillant *et al.* 1999). TIMP-1 in its inducible form has been identified as a multifunction molecule that plays a role in wound healing, regeneration, cell morphology, cell survival, tumor metastasis, angiogenesis, and inflammatory responses (Gardner and Ghorpade 2003). TIMP-1 exerts its neuroprotection

via inhibition of MMPs, which is important for the maintenance of the BBB (Tan *et al.* 2003).

1.5 Regulation of MMP-9 Expression via MAPK-AP1 Signaling Pathways

The goal of this research is to determine what signaling pathways are responsible for increasing the expression of MMP-9 in brain cells and tissue in ischemia and reperfusion. The mitogen-activated protein kinase (MAPK) family is a family of protein kinases and activated by sequential phosphorylation. A number of factors, such as environmental stress, UV light, heat, osmotic shock and inflammatory cytokines trigger the activation of MAPK signaling (Junttila *et al*. 2008). One of the final targeting transcription factors of the MAPK pathways is activator protein-1 (AP-1). Since MMP-9 gene carries two TPA-response elements or AP-1 binding sites in its promoter region, I hypothesize that the ROS generated during ischemia and reperfusion may activate MAPK signaling pathways leading to AP-1 activation by which up-regulates the expression of MMP-9.

The MAP kinase signaling pathways include three distinct groups: extracellular signal-regulated kinases (ERK1/2), c-Jun N-terminal kinases (JNK) and p38 kinases (Whitmarsh and Davis 1996). All of the MAP kinases are activated by dual phosphorylation at threonine (T) and tyrosine (Y) residues in a T-X-Y action motif, where X corresponds to glutamic, proline and glycine for ERK, JNK, and p38, respectively. The ERKs are widely expressed and involved in regulation of cell division processes such as meiosis, mitosis, and post-mitotic function; however, they can also be activated by growth factors, cytokines, or ligands of G-protein receptors (Kolch 2005). ERK was the first of the signaling roadmaps to be characterized whereby ERK is activated by sequential phosphorylation of the upstream kinases Raf and MEK. The activation of Raf occurs through its interaction with membrane-

bound Ras. MAPKKK (MAP3Ks), e.g., Raf, leads to the phosphorylation of MAPKK MEK1/MEK2 which then activate MAPK ERK1/2 that lastly activates AP-1 (Whitmarsh and Davis 1996). JNK (c-Jun N-terminal Kinase) when dually phosphorylated on its tyrosine and threonine residues phosphorylates serine 63 and serine 73 of c-Jun within its N-terminal activation domain. The phosphorylation of the serines in c-Jun causes an increase in AP-1 transcriptional activity. If the serines of c-Jun are not phosphorylated by JNK pathway, c-Jun protein is degraded via the ubiquitin pathway (Manning and Davis 2003). Activation of JNK pathway follows through MEK-1/3→ MAPK kinase (MKK)-4/7 → JNK 1/2/3→AP1. p38 is activated by phosphorylation on its threonine 180 and tyrosine 182. The activation of p38 pathway occurs via MAPK kinase kinase (MAPKKK)→MKK3/6→p38→AP1. The MAP kinases are located upstream of AP-1 signaling pathway. AP-1 is a heterodimeric transcription factor composed of proteins belonging to c-Fos, c-Jun, ATF and JDP families. AP-1 is activated by TPA (12-O-tetradecanoyl phorbol-mycetate-acetate), phorbol esters, growth factors, cytokines and oncoproteins (Whitmarsh and Davis 1996). AP-1 activated by MAPK signaling pathways is translocated to the nucleus where it binds to the promoters of target genes containing the TPA response element (i.e., AP-1 binding site) and attaches to DNA via its leucine zipper domain.

Research in recent years has suggested that MAPK signaling pathways and AP-1 could be involved in MMP-9 up-regulation. In a rat brain astrocytes model, treatment with oxidized low-density lipoprotein (oxLDL) induced proMMP-9 expression which was thought to be mediated through JNK1/2 and ERK1/2 pathways leading to AP-1 activation (Wang *et al*. 2009). In cortical neuronal cultures, ERK1/2 was rapidly and transiently phosphorylated

upon oxygen and glucose deprivation (Boulous *et al.* 2007). Sustained ERK1/2 phosphorylation was found to be required but not sufficient for MMP-9 expression (Genersch *et al.* 2000). PMA-induced rat astrocytes showed phosphorylation of all three MAPK pathways but only treatment with an ERK1/2 specific inhibitor significantly reduced MMP-9 up-regulation (Arai *et al.* 2003). In addition, recent works show that inhibition using an ERK inhibitor U0126 ameliorated the degradation of the tight junction protein zona occludens 1 (ZO-1) and significantly decreased edema, indicating that ERK-MAPK pathway may trigger the up-regulation in MMP-9 after trauma (Mori *et al*. 2002). In a human squamous cell line, cancer research revealed that p38 MAPK and its downstream target MAPK2 is strongly activated by treatment with a phorbol ester (Simon et al. 1998). Research on invasiveness in cancer has suggested a link between MKK-6, p38 isoforms, AP-1 and MMP-9 (Simon *et al.* 2001). Other research findings have shown the link between MMP-9 and AP-1: 1) Blockage of AP-1 components c-Fos and c-Jun improved neurological outcome in rats (Dai *et al.* 1999); 2) Linoleic acid hydroperoxide (LHP) was shown to increase AP-1 activity and up-regulate MMP-9 gene response in the rabbit retina (Iwai *et al.* 2006); and 3) Inhibition of AP-1 with silibinin reduced PMA-induced MMP-9 expression in MCF-7 human breast carcinoma cells (Lee *et al.* 2007).

Given the abovementioned research, it seems likely that MAPK signaling pathways activate AP-1 and play a role in up-regulating MMP-9 expression. Given this premise, blockage of MAPK signaling pathways may decrease the expression of MMP-9 and relieve oxidative stress-induced MMP-9 expression and consequential blood-brain barrier (BBB) damage following cerebral ischemia and reperfusion.

Although MMP-9 plays a significant role in the pathology of ischemic stroke, whereby it aides in the detrimental breakdown of the blood-brain barrier, the signaling required for MMP-9 up-regulation has yet to be fully elucidated in ischemic stroke. Since MCP-1, VEGF and ROS are generated in ischemic stroke, it is important to understand whether these factors affect MMP-9 expression and its activity and the signaling pathways involved. In this current study, my objective is to provide insight into the molecular regulatory mechanisms of MMP-9 up-regulation induced by oxidative stress generated during hypoxia/ischemia and reoxygenation and to show a change in the expression of MMP-9 in a rat astrocyte cell line (NRA) by activation of JNK, ERK and p38 MAP kinase signaling pathways that converge onto transcription factor AP-1. The ultimate goal of the research is to modulate MMP-9 expression and activity to reduce BBB permeability.

1.6 Research Proposal

1.6.1 Hypothesis

I hypothesize that reactive oxygen species (ROS) or oxidative stress will up-regulate MMP-9 expression via MAPK-AP1 signaling pathway in astrocytes which contributes to BBB disruption. The main objective of this research is to provide insight into the molecular regulatory mechanisms of MMP-9 expression and to modulate MMP-9 expression and activity which could be used in future studies to reduce MMP-9 mediated damage to the blood-brain barrier (BBB) and consequent brain damage associated with increased permeability.

1.6.2 Objectives

1. Develop an *in vitro* model that mimics oxidative stress in ischemic stroke.
2. Characterize the gene and protein expression as well as the catalytic activity of MMP-9 in the *in vitro* model.
3. Up-regulate MMP-9 expression *in vitro* by activating MAPK and AP-1 signaling pathways.
4. Inhibit the expression of MMP-9 *in vitro* by blocking the relevant signaling pathways (MAPK and AP-1) and characterize changes in gene, protein and catalytic activity.
5. Clone the AP-1 binding site from human MMP-9 gene and characterize the effects of my *in vitro* model in the presence/absence of MAPK inhibitors on AP-1 reporter gene activity.
6. Down regulate MMP-9 expression by MAPK inhibitors and test the effect on permeability of an *in vitro* model of the blood-brain barrier.
7. Clone and purify a TIMP-1 fragment for use as an endogenous inhibitor of MMP-9 activity for future studies.

Chapter 2: Materials and Methods

2.1 Chemical and biochemical reagents

Dulbecco's modified Eagle's medium (DMEM), M199 phenol free medium, Antibiotic/Antimycotic, Hank's balanced salt solution (HBSS), trypsin, reverse transcriptase MLV enzyme, TaqDNA polymerase, restriction enzymes, Trizol reagent, LipoFectamine 2000, ultraPure distilled RNase- and DNase-free water were purchased from Invitrogen (Burlington, ON). Fetal bovine serum (FBS) was purchased from Hyclone (Logan, UT). Hydrogen Peroxide (H_2O_2), Fluorescein (F6377), Phorbol 12-Myristate 13- Actetate (PMA), Anti-ß-Actin monoclonal antibody (mAb), protease inhibitor cocktail, dimethyl sulfoxide (DMSO), Triton X-100 and Tween-20 were purchased from Sigma (Oakville, ON). Phospho p38 (Thr180/Tyr182) MAP kinase mAb, p38 MAP kinase mAb, Phospho-p44/42 MAPK (ERK1/2) (Thr202/Tyr204) mAb, p44/42 MAPK (ERK1/2) mAb, Phospho-c-Jun (Ser63) II mAb, Phospho-c-Jun (Ser73) II mAb, and c-Jun (60A8) mAb were purchased from Cell Signaling (Danvers, MA). Anti-MMP-9 Catalytic Domain mAb and Anti-MMP-9 were purchased from Millipore (Temecula, CA). Goat-Anti-Rabbit-IgG Secondary Antibody was purchased from Santa Cruz Biotechnology (Santa Cruz, CA). Anti-rabbit secondary antibody conjugated with Alexa 568 was purchased from Molecular Probes/Invitrogen (Burlington, ON). Western blotting stripping buffer was purchased from Pierce Biotechnology/Fisher Scientific (Nepean, ON). ECL plus Western blotting detection kit was purchased from Amersham/Pharmacia Biosciences (Montreal, QC). Precast Zymogram Gels, Zymograph Buffers, PVDF Membrane, BioRad DC Protein Assay kit and Precision plus protein standards were purchased from Bio-Rad (Mississauga, ON). Tricholoroacetic acid was purchased from Fisher Scientific (Nepean, ON). Plasmid DNA purification kit and

Omniscript Reverse Transcription kit were purchased from QIAGEN (Mississauga, ON). SYBR Green PCR Master Mix Kit was purchased from Applied Biosystems Inc (Foster City, CA). Luciferase Assay Kit was purchased from Promega/Fisher Scientific (Nepean, ON). SP600125, an inhibitor of Jun N-terminal kinase (JNK) was purchased from Caliochem, Inc. SB 203580, an inhibitor of MAP kinase homologues p38α, p38ß, and p38ß2, and a MEK inhibitor U0126 were purchased from Promega (Madison, WI). An inhibitor of p38 MAP kinase PD 169316 and an inhibitor of ERK2 CAY10561 were purchased from Cayman Chemicals (Burlington, ON). Recombinant rat proteins monocyte chemoattractant protein- 1 (MCP-1) and vascular endothelial growth factor (VEGF) were purchased from PeproTech (Rocky Hill, NJ). Recombinant human MMP-9 (catalytic domain) and MMP-9 chemical inhibitor SB-3CT were purchased from Enzo Life Sciences (Plymouth, Pennsylvania). Specialized BD Falcon cell culture plates and 1.0 µM pore size culture inserts were purchased from VWR International (Mississauga, Ontario).

2.2 Cell Culture

Neonatal rat astrocytes (NRA) were generated from the cortex of 4-8 day old neonatal Sprague-Dawley rats isolated in house and then immortalized with SV40 large T antigen. The immortalized NRA cells were provided by Dr. D. Stanimirovic at the NRC-Institute for Biological Sciences. Passages 77 to 84 were used in the experiments of this study. NRAs were maintained in DMEM supplemented with 10% FBS and 1% antibiotic/antimycotic. The medium was changed every second day and cells were plated at an appropriate density according to each experimental scale. HEK293 cells (human embryonic kidney epithelial cells) were maintained in DMEM with 10% FBS, medium was changed every second day and cells were plated at appropriate density for transfection protocol. Immortalized rat brain

microvascular endothelial cells (SV-ARBEC) passages 78-82 were used in the *in vitro* model of the BBB for permeability test. SV-ARBEC cells were maintained in M199 medium supplemented with 10% FBS as described previously (Zhang *et al*., 2003). Cells were cultured on semi-permeable 1.0 μM pore membrane inserts that were coated with rat-tail collagen (60 μg/mL) for 1 h before plating. SV-ARBEC cells were grown for 6 days without feeding to allow a tight monolayer of cells to form.

2.3 RNA isolation, RT-PCR, and Real-time quantitative PCR

NRA cells were treated with H_2O_2 (0.5, 1.0, and 2.0 μM), MCP-1 and VEGF (200 and 400 ng/mL), PMA (1.0 μM) or their respective vehicles H_2O, 0.1% BSA in H_2O or DMSO for 2, 4, and 6 h, respectively. Total RNA was isolated from cultured cells using TRIzol reagent following the manufacturer's instructions. TRIzol reagent lysed the cells and the lysates were transferred to 1.5-mL tubes. Chloroform was added and the samples were shaken for 30 seconds. The mixtures were settled for 2 min and centrifuged at 14, 000 rpm (18, 000 g) for 15 min at 4^{o}C. Clear supernatants were transferred to 1.5-mL tubes followed by addition of equal volume isopropanol and then vortex. RNA was left to precipitate overnight at -20^{o}C. After warming up to room temperature, the mixture was centrifuged at 10, 000g for 10 min at 4°C, and RNA was precipitated as a pellet in the tube. The pellet was washed one time with 70% ethanol in ultraPure DNase-and RNase-free H_2O. RNA pellets were resuspended in ultraPure DNase-and RNase-free H_2O and heated to 55^{o}C for 10 min. RNA concentration was read at 260 OD values for each sample using NanoDrop 1000 UV-Vis Spectrophotometer (Thermo Scientific Inc., Nepean, ON).

For reverse transcriptase (RT) reaction, 2 µg RNA was pre-heated with 1 µg Oligo (dT) primers at 70^{o}C for 10 min. After cooling on ice, 5x first strand buffer, 10 mM dNTP, 0.1 M DTT and 50 units of MLV reverse transcriptase were added to the reaction mix and incubated at 42^{o}C for 2 h according to manufacturer's instructions. For a negative control, RT reaction was performed on a chosen sample as described above with the exception of RNase/DNase-free dH_2O instead of MLV reverse transcriptase. Specific DNA sequences were amplified using PCR master reaction mixture, including 10x PCR buffer, 10 mM dNTP, 1.5 mM $MgCl_2$, 10 µM primer cocktail, 1.25 units/reaction Taq polymerase, cDNA and RNase/DNase-free dH_2O. All PCR primers (Table 1) were designed according to published sequences in the GenBank and synthesized by the Alpha DNA (Montreal, Quebec). Six-time loading buffer was added to amplified products and samples were loaded (20 µL/lane for MMP-9 and 10 µL/lane for ß-actin) on 1.5 % agarose gel in 1x TBE buffer both containing 0.5µg/mL ethidium bromide. PCR products were resolved on 1.5% agarose gel by electrophoresis at 100V for 50 min. The gels were exposed using UV light on Alpha Innotech FluorchemQ system (Santa Clara, California). DNA bands for β-actin and MMP-9 from RT-PCR reactions were quantified using densitometry analysis software UN-SCAN-IT gel TM Version 6.1 software (Silk Scientific Inc., Orem, Utah). The numerical values given for the β-actin and MMP-9 bands taken from the gel images represented number of dark spots in a given area found in each band from the gel photographs. Final values used to plot bars on graph were determined by taking numerical value of MMP-9/β-actin ratios and comparing as fold change of stimulus vs. vehicle treated cells.

For real-time quantitative PCR, RNA was converted to cDNA using Omniscript kit (Qiagen) according to manufacturers' instructions. For RT reaction, 2 µg RNA was added to

a total volume of 20 µL RNase/DNase-free dH_2O and pre-heated to 65^oC for 5 min. After cooling on ice, 10 x buffers, 5 mM dNTP, 10 µM Oligo-dT, RNase inhibitor 10 units/µl and Ominiscript Reverase Transcriptase 1µL/reaction were added to the reaction mix and incubated at 37^oC for 1.5 h according to manufacturer's instructions. For q-PCR reaction, cDNA was diluted 1/10 and then SYBR green and 5µM of sense and anti-sense primers were added to the mixture. The plate was covered with optical adhesive strip, spun down gently and placed in ABI Prism Optical qPCR Machine and run based on manufactures instructions.

Table 1. PCR Primers used in the study

Gene	Primer Sequences	
β-actin (RT-PCR)	Sense	5'-GGCTACAGCTTCACCACCAC-3'
	Anti-Sense	5'-TACTTCCGCTCAGGAGGAGC-3'
MMP-9 (RT-PCR)	Sense	5'-CAG AGT CTT CGA CTC CAG TAG-3'
	Anti-Sense	5'-ACG TGG TCC ACC TGG TTC AC-3'
β-actin (QPCR)	Sense	5'-TGTCCACCTTCCAGCAGATGT -3'
	Anti-Sense	5'-AGTCCGCCTAGAAGCATTTGC-3'
MMP-9 (QPCR)	Sense	5'-GTTTCCACAACCGGGTGAAC -3'
	Anti-Sense	5'-GCACCGCTGAAGCAAAAGA -3'

2.4 Western blot analyses

Confluent NRA cells grown in 12-well culture plates were treated with 0.5, 1.0, and 2.0 µM H_2O_2 for 2, 4, and 6 h, respectively. The cells were washed 2 times in colour-free HBSS and then were lysed in loading buffer. After 10 min shake, the cells were scraped off and transferred to 1.5-mL tubes. The lysates were then vortexed and put on ice for 3 min, boiled at 100˚C for 10 min, cooled and centrifuged at 14,000 rpm (18, 000 g) for 10 min at 4˚C. Protein concentration was determined using trichloroacetic acid (TCA) protein assay. TCA assay was performed on 96-well plate where known concentration of bovine serum albumin

(BSA) was used as a standard curve to generate protein concentrations, from 10 μL of each sample done in duplicate. TCA was added to generate reaction, and the plate was incubated for 15 min until yellowish color developed and was then read by Spectra MAX 340 spectrophotometer under 570 nm (Molecular Devices Inc.) using SoftMax PRO program. Equal micrograms of protein were loaded on 10% SDS-PAGE gel. Proteins were transferred to PVDF membrane sandwiched in western blot transfer unit and ran at 150 mA overnight. Blots were blocked for 1 hour at room temperature in fresh blocking buffer [0.1 % Tween-20 in Tris-buffered saline (TBST), pH 7.4, containing 5% non-fat dried milk). At dilutions of 1:1000, primary antibodies of Phospho p38 (Thr180/Tyr182) MAP kinase mAb, p38 MAP kinase mAb, Phospho-p44/42 MAPK (ERK1/2) (Thr202/Tyr204) mAb , p44/42 MAPK (ERK1/2) mAb, Phospho-c-Jun (Ser63) II mAb, Phospho-c-Jun (Ser73) II mAb and c-Jun (60A8) mAb (Cell Signaling) and Anti-MMP-9 Catalytic Domain mAb (Millipore) were made up of 0.1% TBST containing 1% non-fat dried milk and the blots were incubated overnight at 4°C. Following three washes in 0.1% TBST, the blots were incubated with 1:5000 secondary antibodies conjugated with horseradish peroxidase (donkey anti-rabbit IgG) (Santa Cruz Inc) for 1 h at room temperature. Blots were washed again three times with 0.1% TBST and were subsequently developed using ECL Plus substrate solution for 5 min according to manufacturer's instructions and visualized using X-ray film.

2.5 Gelatin Zymography for MMP-9 Activity in Astrocyte-Conditioned Media

Confluent NRA cells grown in 12-well culture plates were treated with 0.5, 1.0, and 2.0 μM H_2O_2 in the presence or absence of a pharmacologic inhibitor. After treatment, the conditioned media were collected, spun down by 10,000 rpm (9,000 g) centrifugation and mixed with equal amount non-reduced sample buffer (BioRad). Samples were loaded on a

10% gelatin SDS gel (precast by BioRad) and electrophoresed for 90 min at 100 V. Mixed blend of collagenases (Sigma) was used as a protein standard and positive control. Cell lysates were washed 1 time in colour-free HBSS and lysed in RIPA buffer for normalization with BioRad Protein Assay. BioRad protein assay was performed in 96-well plate where 2 mg/mL BSA was added in known amounts diluted with H_2O providing a standard curve. Protein concentration was determined using BioRad DC Protein Assay kit (BioRad Laboratories Inc., CA). Protein assay was performed on 96-well plate format by initially establishing a standard curve using 2 mg/mL BSA and serially diluting it in H_2O and spiking it with RIPA buffer. Each sample was added to the plate, diluted in H_2O and then received mixture of Reagent A and S, followed by addition of reagent B obtained from the kit. Plate was placed on a shaker for 15 min until bluish colour developed and was subsequently read by Spectra MAX 340 spectrophotometer under 750 nm (Molecular Devices Inc.) using SoftMax PRO program.

2.6 MMP-9 Activity Assay

Confluent NRA cells in 24-well culture plates were pretreated with a pharmacologic inhibitor of MAP kinases at concentration of 20 μM for 30 min. After pretreatment, H_2O_2 was added to full culture media to final concentrations of 0.5 and 1.0 μM. H_2O_2 was left for 30 min, then media were switched for DME with 1% FBS for 2, 4, and 6 h. After treatment, conditioned media were collected, spun down by 10,000 rpm (9,000 g) centrifugation. Cell lysates were washed one time with colour-free HBSS and lysed in RIPA buffer for normalization with BioRad Protein Assay. MMP-9-containing conditioned media were added to black 96-well plates. For every sample, 50 μL was added in triplicate and then 50 μL of warmed component D (Fret-peptide/ flourogenic substrate) was added. Plate was

immediately placed into BioTek FLx800 Fluorescence Microplate Reader (Winooski, VT); readings were taken every 5 min for 1 h. Readings were normalized to 1% FBS DME media and reported as fold change in fluorescence.

2.7 Immuncytochemistry

NRA cells were plated at 80, 000 cells/mL in 24-well culture plates until reached 75% confluence. The cells were treated for 4 h with 1.0 μM H_2O_2 in regular culture media in the presence or absence of a pharmacologic inhibitor of MAP kinases at 20 μM. Media were aspirated; cells were washed 1 time in colour-free HBSS solution and then fixed by addition of ice-cold methanol for 5 min. Cells were washed in 4 times with HBSS. After ensuring integrity of the cells, they were permeablized with the addition of 0.1% Triton X-100 for 10 min at room temperature. Cells were washed in 3 times with HBSS for 5 min each. Cells were then blocked with 4% normal goat serum in HBSS for overnight at 4°C. Primary MMP-9 antibody was then added at 1/100 dilution in 1% goat serum overnight at 4°C, and for secondary alone, control 1% goat serum in HBSS was added. Cells were washed in 2 times with HBSS before the addition of secondary Alexa568-conjugated anti-rabbit antibody at 1/500 dilution in HBSS, and the cells were incubated for 30 min at room temperature in the dark. Cells were then washed 3 times in HBSS before the addition of Hoechst 33342 at 1/5000 dilution in HBSS for 15 min. Images were taken with fluorescent microscope Olympus 1X81 (Center Valley, Pennsylvania) at 10x and 20x magnification.

2.8 Transient transfection and AP-1 reporter gene luciferase assay

HEK293 cells were plated at 50,000 cell/well in 48-well plates or 100 000 cell/well in 24-well plates 24 h before transfection at which point they were 80 % confluent. HEK293 cells

were transiently transfected with a reporter gene vector construct that contains AP-1(2) binding insert (Panomics Inc) or AP-1 binding insert cloned from human MMP-9 gene promoter region into pGL-3 basic vector (Promega Corp.) using LipoFectamine transfection reagent (2:1 ratio of reagent to plasmid in µg). After 48 h recovery period at 37˚C, cells were treated with 1.0 µM PMA, 1.0 µM H_2O_2 or vehicle for 30 min, 2, 4, 6, and 24 h. The 30-min time point was determined to be the best for AP-1 activation by H_2O_2. After treatment cells were lysed in 1x cell lysis buffer provided in the Luciferase assay kit and spun down at 10,000 rpm for 2 min. Luciferase assay was performed using a kit purchase from Promega Co., (Cat# E1500, Madison, WI, USA). For luciferase assay, 20 µL of each sample was added to a black 96-well plate and 100 µL of luciferase enzyme was added by plate reader injector. Luminescence units were determined using BioTek FLx800 Fluorescence Microplate Reader (Winooski, VT). Luciferase units were normalized to protein in µg protein per sample using BioRad DC protein assay reagents previously described. HEK293 cells were used for reporter gene assay experiments due to low transfection efficiency in NRA cells (<5%).

2.9 Blood-Brain Barrier in vitro Assay

An *in vitro* Blood-Brain Barrier (BBB) model was cultured using SV-ARBEC cells and conditioned media collected from confluent NRAs. On day one of the experiment, cell culture inserts were coated with rat tail collagen at 60 µg/mL and SV-ARBEC cells were plated at the density of 80, 000 cells/mL. A 1:1 ratio of complete M199 phenol red free SV-ARBEC medium was mixed with DME phenol red free 1% FBS, NRA conditioned media (72 h off NRA confluent cells). Cells were incubated at 37°C for 6 days with no feeding for cells to form a tight monolayer. Before the experiment was done, the monolayer was tested

for its permeability coefficient (Pe) with sodium fluorescein to ensure proper amount of *in vitro* transport across the *in vitro* BBB from the top chamber into the bottom chamber. In order to calculate Pe, culture inserts were gently lifted and washed 3X in warmed HBSS clear, and then placed in warmed 1X transport buffer. A known concentration of sodium fluorescein (50 µg/mL) was mixed 1:1 with pre-existing SV-ARBEC media, resulting in a final concentration of 25 µg/mL in the upper chamber. The plate was then placed into a shaking incubator at 37ºC. At time intervals of 15, 30, 45, 60, 90 and 120 min, 100 µL of transport buffer was removed from the bottom chamber, and 100 µL of fresh transport buffer was added. For inserts without SV-ARBEC cells, the same protocol was used with the exception of time intervals of 3, 7, 10, 15 and 20 min periodically during and after the experiment had been completed, the cell monolayers were checked under the microscope to ensure no folding or loss of cells indicating disrupted membrane integrity. After all of the time points had been collected, the 100 µL for each time point was added to a 96-well black plate and read in the plate reader at an excitation of 485 nm and an emission of 580 nm. After the Pe had been calculated as being between the standard rates for permeability generally between 0.5-0.8 X $10^{\text{-}3}$ cm/min, different treatments were added to the cells with a known concentration of sodium fluorescein and permeability was tested. The different treatments include: active MMP-9, active MMP-9 + MMP-9 inhibitor (SB-3CT), H_2O_2 at 1.0 µM in NRA media, and conditioned media from NRA experiments where H_2O_2 had been treated for 4 h at 1.0 µM H_2O_2 and their respective vehicles. Standard curves were then used to calculate the amount of sodium flourescein passing through the membrane, indicating the effect of treatments on BBB permeability. Once all time points were recorded, the permeability's were compared to determine if treatment disrupted membrane integrity.

2.10 Statistical analysis

Data were presented as mean ±SD. Statistical analysis for single comparison was performed by unpaired or paired Student's *t*-test where each experiment was repeated at least 3 times (n=3). Statistical analysis for group comparison where one factor was being analyzed was performed by one-way ANOVA with Dunnett's post-test where each experiment was done at least 3 times (n=3). The criterion for statistical significance was $p<0.05$. Statistical analysis for group comparison where two factors were being analyzed was performed by two-way ANOVA where each experiment was done at least 3 times with Bonferroni's post-test (n=3). The criterion for statistical significance was $p<0.05$.

Chapter 3: Results

3.1 Development of an in vitro model of MMP-9 up-regulation

3.1.1 AP-1 agonist PMA induces MMP-9 gene expression via MAP kinase pathways and Activator Protein-1.

The first objective of this research was to develop a model to test the signaling pathways of MMP-9. Seven cell lines and six different stimuli were tested to develop a consistent, biologically relevant model in which there was significant up-regulation in expression of MMP-9 (Table 2). Although under some of the treatment conditions MMP-9 was detectable, it was not in significant levels to test the effect of inhibitors or modulate expression. Preliminary experiments were done using a known AP-1 agonist PMA as the stimulus to induce MMP-9 expression in the neonatal rat astrocytes (NRA). NRAs treated with 1 μM PMA resulted in an increase in the expression of MMP-9 compared to controls at 6 h (Figure 3). Gene expression was normalized using β-actin. Gene expression showed an increasing trend from 2 h to 6 h of treatment. DME media with 0.01% DMSO represent the internal control for PMA treatment and did not significantly affect MMP-9 gene expression in NRAs. The addition of a pretreatment with MAPK inhibitors for p38 kinase showed a significant reduction in MMP-9 gene expression (Figure 4). Gene expression was normalized using β-actin. DME media with 0.06% DMSO represent the internal control for inhibitor treatment and did not significantly affect MMP-9 gene expression in NRAs. This suggests that p38 MAP kinase pathway is involved in the regulation of MMP-9 gene expression. MAP kinase pathways have been shown to converge on AP-1, which can induce gene transcription. I hypothesized that AP-1 may induce MMP-9 gene expression, as PMA is a known AP-1 agonist. To confirm this finding, reporter gene assays were performed

using AP-1 binding sites from the MMP-9 human promoter region. The human MMP-9 gene has two AP-1 binding sites in the promoter region (Figure 5). The two binding sites were cleaved and inserted into pGL-3 reporter gene vector (pGL-3/AP-1). Results confirmed that treatment with PMA at 1.0 μM for 24 h led to significantly greater luminescence than vehicle (Figure 6 Panel A). Internal control showed pGL-3/AP-1vector has significantly greater luminescence than empty pGL-3 vector under all treatment conditions (Figure 6 Panel B). This result demonstrates that AP-1 transcription factor is stimulated by PMA and that this could be the mechanism of how MMP-9 gene expression is activated. The preliminary results show that I can induce MMP-9 gene expression in NRA cells and that MAP kinase pathways and AP-1 transcription factor play a role in the increase in expression. The preliminary findings of this study were used to establish a working cell culture model and in later experiments PMA was used as a positive control in establishing a more biologically relevant stimulus.

Table 2. Cell lines and stimuli tested to find a biologically relevant in vitro model.

Cell Line	Stimulus	Detection Method	MMP-9 Result
Immortalized Human Brain Endothelial (iHBEC)	Hypoxia Chamber/PMA/MCP-1/VEGF	RT-PCR & WB	Negative
Human Astrocytes	PMA	RT-PCR	Positive
Human Microglial (C13NJ)	Hypoxia Chamber/PMA/CoCl2	RT-PCR & WB	Negative
Human Umbelical Vein Endothelial Cells (HUVEC)	Hypoxia Chamber	RT-PCR	Negative
Human Brain Endothelial Cells (HBEC)	MCP-1/VEGF	q-PCR	Negative
Rat Endothelial Cells (SV-ARBEC)	MCP-1/VEGF/PMA	RT-PCR	Positive
Neonatal Rat Astrocytes (NRA)	MCP-1/VEGF/PMA/H202	RT-PCR	Positive

A)

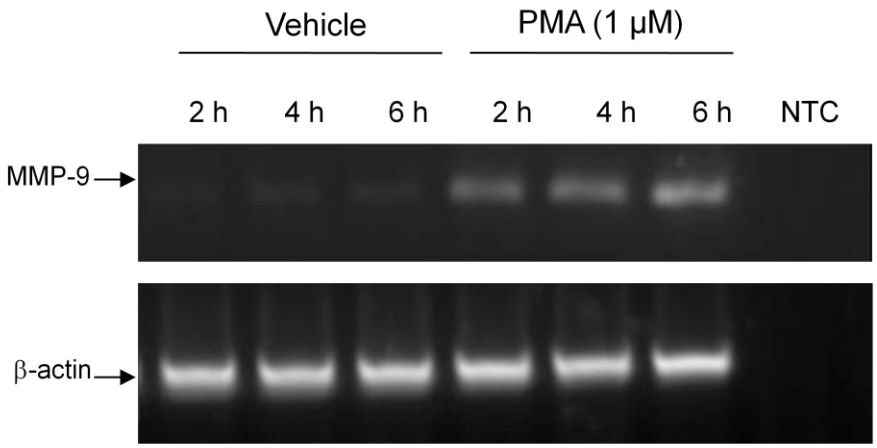

B)

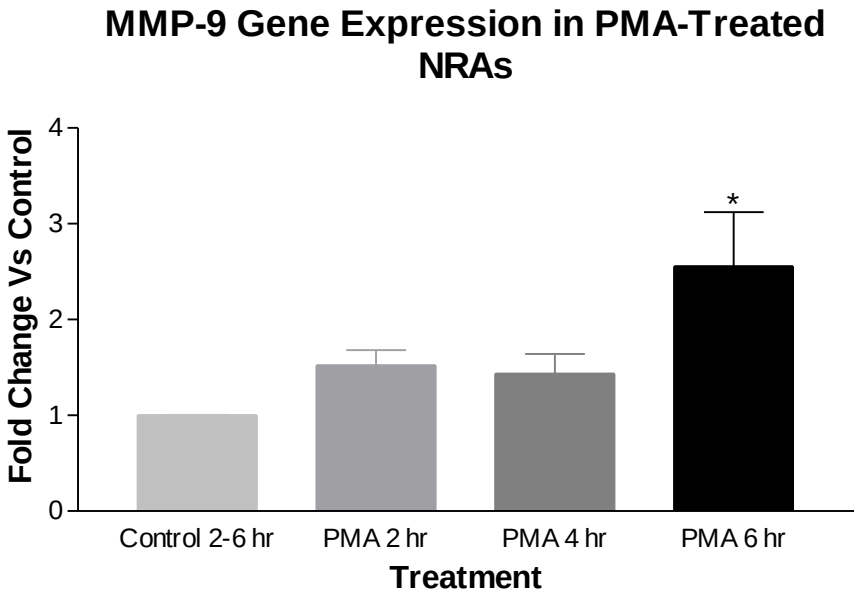

Figure 3. RT-PCR to detect the effect of PMA on MMP-9 gene expression in astrocytes (NRA).

Panel A) RT-PCR shows MMP-9 gene expression in NRA cells following treatment with an AP-1 agonist PMA at 1.0 µM for 2, 4, and 6 h. **Panel B)** Densitometry analysis demonstrates MMP-9 expression is significantly higher at 6 h in PMA-treated cells than the vehicle (N=3, One-way ANOVA with Dunnett's post-test, F (2,8), 4.459, * $p<0.05$). ß-actin was used as an internal control. NTC: negative control for RT-PCR.

A)

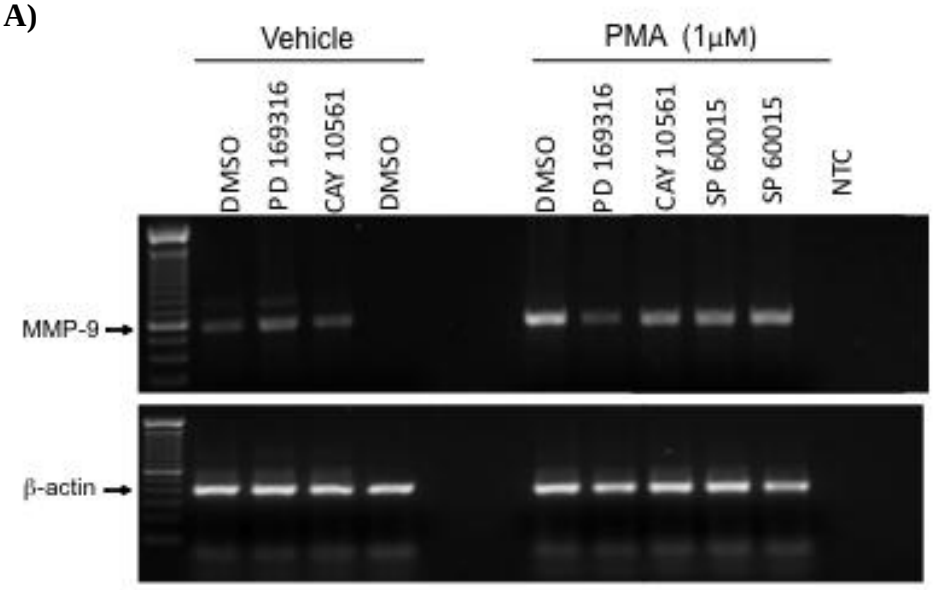

B)

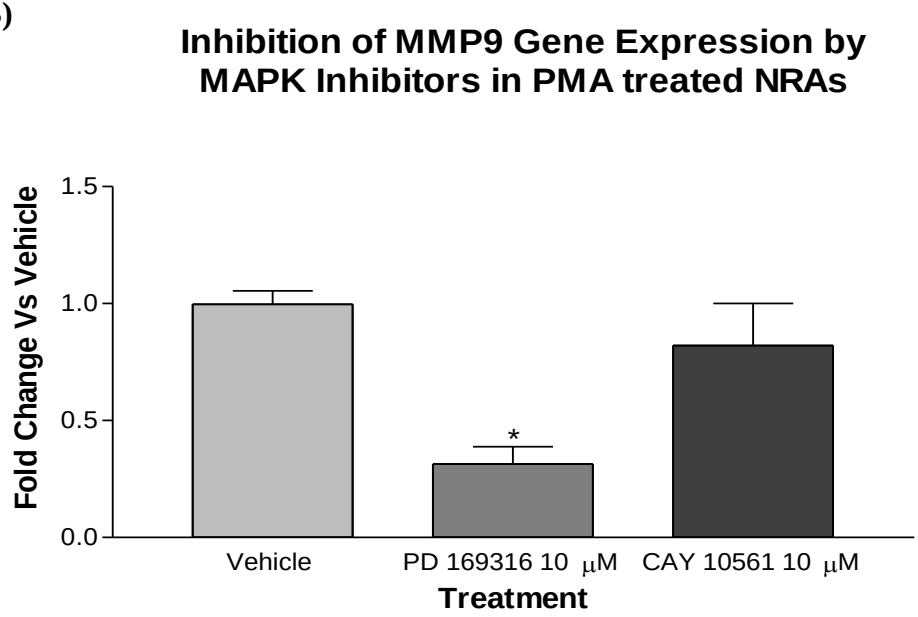

Figure 4. RT-PCR to detect the effect of MAPK inhibitors on MMP-9 gene expression in astrocytes (NRA) treated with PMA.

Panel A) RT-PCR shows MMP-9 gene expression in NRA cells following pretreatment with vehicle, 10 μM of p38 MAPK inhibitor PD 169316, ERK2 inhibitor CAY 10561 and JNK Inhibitor SP600125 followed by 1 μM PMA treatment for 4 h. **Panel B)** Densitometry analysis shows MMP-9 expression is reduced by a p38 kinase inhibitor (N=3, *t*-test, $p<0.05$). β-actin was used as an internal control. NTC: negative control for RT-PCR. JNK treatment (N=1)

A)

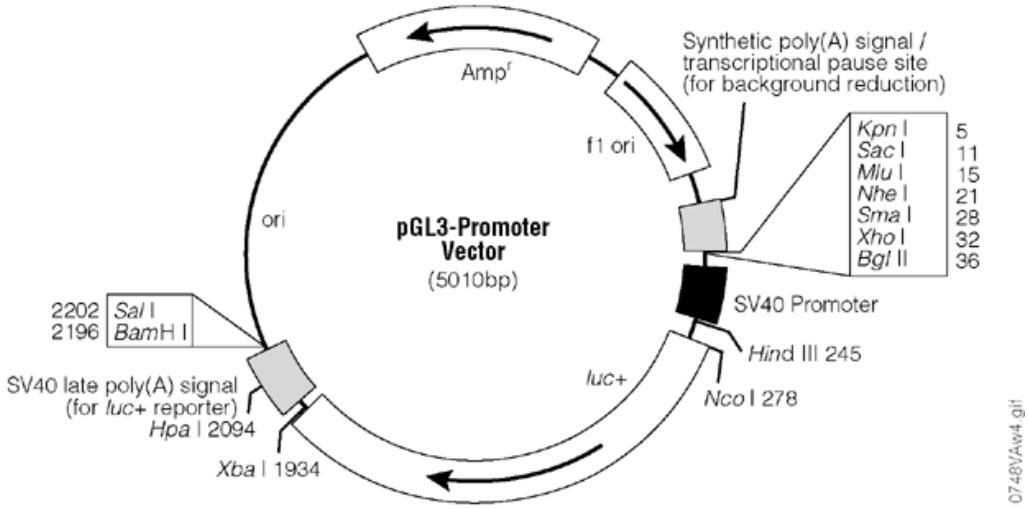

MMP9/AP1/NheI/foreword:
5'-CTAGCTAGCTAGGATGAAGCAGGGAGAGGAAG-3'

B)

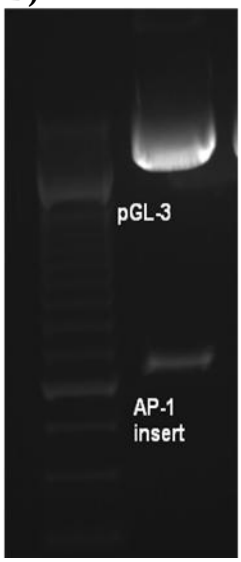

Figure 5. Cloning AP-1 binding site from human MMP-9 gene and luciferase reporter gene assay.

Panel A) An AP-1 binding site from MMP-9 gene and its cloning into pGL3-basic vector. **Panel B)** Restriction and sequencing analysis confirm AP-1 is cloned into the pGL-3 vector.

A)

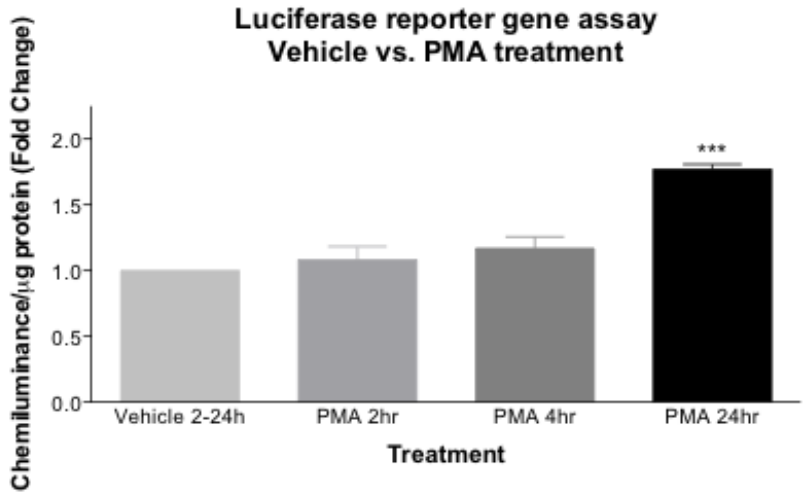

B)

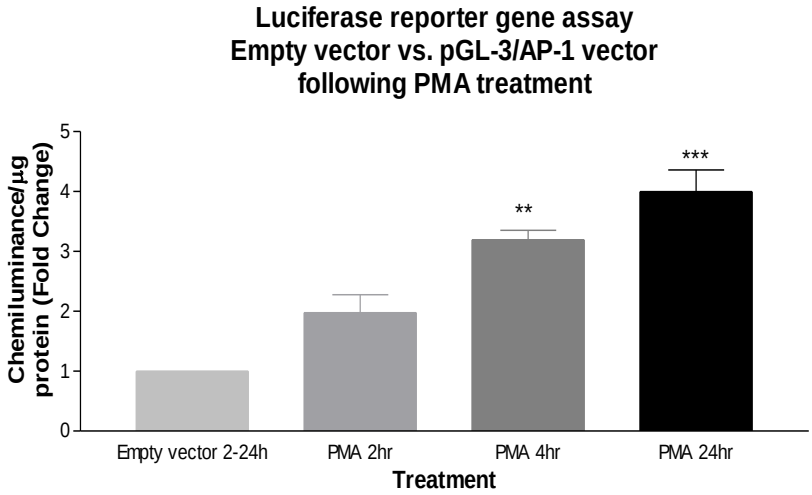

Figure 6: Reporter Gene Assay for effect of PMA on AP-1 Transcriptional Activity. **Panel A)** HEK293 cells were transfected with pGL-3/AP-1 vector and then treated with vehicle or PMA for 2, 4, and 24 h. PMA strongly stimulated reporter gene activity at 24h treatment (N=3, One-way ANOVA with Dunnett's post-test, $F_{3,9} = 32.58$, ***p<0.001). **Panel B)** HEK293 cells were transfected with an empty pGL-3 vector or pGL-3/AP-1 vector and then treated with PMA for 2, 4 and 24 h, respectively. The AP1 promoter was strongly activated by PMA treatment at 4 and 24 h compared to the empty vector (N=3, One-way ANOVA with Dunnett's post-test, $F_{3,9}=23.41$, **p<0.01, ***p<0.0001).

3.1.2 MCP-1 and VEGF show no significant effect on MMP-9 gene expression in astrocytes

As mentioned previously, the goal was to establish a more biologically relevant stimulus for testing MMP-9 gene expression in astrocytes. Since both MCP-1 and VEGF were highly produced during ischemic stroke, the two cytokines were tested in NRA cells for 2, 4, and 6 h and analyzed by RT-PCR. Densitometry analysis of PCR data found that there was no significant change in MMP-9 gene expression given this treatment dosage and time course (Figure 7). Gene expression was normalized using β-actin. DME media with 0.1% BSA represent the vehicle internal control for recombinant MCP-1 and VEGF treatment and did not significantly effect MMP-9 gene expression in NRAs. Although the results suggest a trend of increasing MMP-9 gene expression, additional experiments were not pursued, as hydrogen peroxide experiments were being undertaken at the same time and proved to be an effective stimulus for the project.

A)

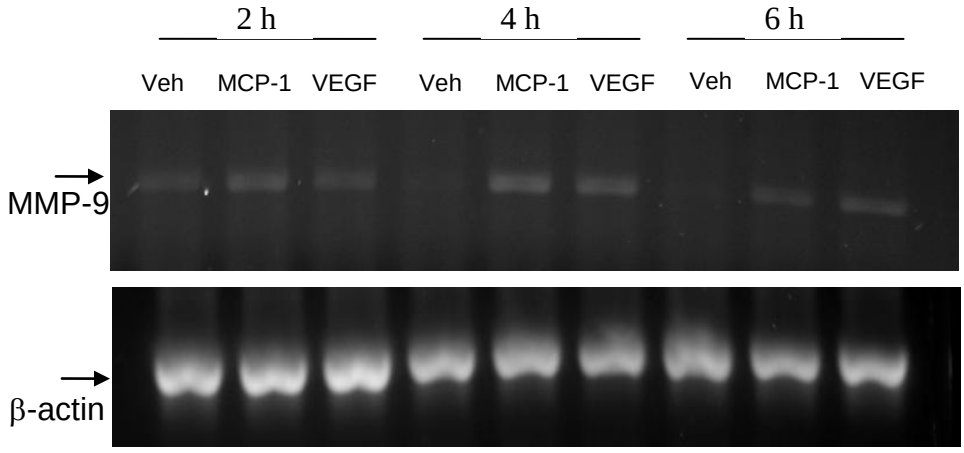

B)

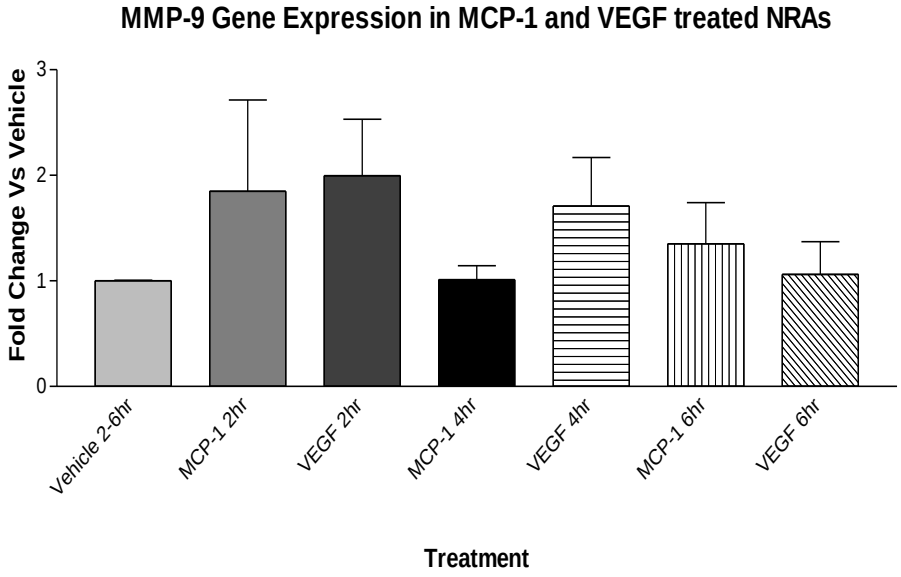

Figure 7: RT-PCR to detect the effect of MCP-1 and VEGF on MMP-9 gene expression in astrocytes (NRA).

Panel A) RT-PCR shows MMP-9 gene expression in NRA cells following treatment with Vehicle, 200 ng of MCP-1 and VEGF for 2, 4, and 6 h. **Panel B)** Densitometry analysis shows MMP-9 expression is trending higher in MCP-1 treated cells at 2 h and VEGF treated cells at 2 h and 4 h (N=3, One-way ANOVA, $p>0.05$). β-actin was used as an internal control. NTC: negative control for RT-PCR.

3.2 Characterization of H_2O_2 - Induced Oxidative Stress on MMP-9 Expression

3.2.1 H_2O_2 - Induced Oxidative Stress increases MMP-9 gene expression in Astrocytes

Treatment of NRA cells with H_2O_2 at 0.5, 1.0, and 2.0 µM for 2, 4, and 6 h was analyzed using RT-PCR (Figure 8). Densitometry results show a significant increase in the mRNA level of MMP-9 in H_2O_2 treated NRAs. Gene expression was normalized using β-actin. The increase in gene expression is shown to peak with treatment of H_2O_2 at 1.0 µM for 4 h. DME medium with H_2O represents the vehicle internal control for H_2O_2 treatment and did not significantly affect MMP-9 gene expression in NRAs. The RT-PCR result was confirmed by real-time quantitative PCR, which confirmed 1.0 µM treatment for 4 h results in the greatest increase of MMP-9 gene expression (Figure 9). Gene expression was normalized using β-actin.

3.2.2 H_2O_2 - induced oxidative stress decrease MMP-9 parent protein expression in astrocytes

To further understand the effect of H_2O_2 on MMP-9 expression, western blotting was done for the same treatments to show the effect on pro-MMP-9 (parent protein) expression. Treatment of NRA cells with H_2O_2 at 1.0 and 2.0 µM for 2, 4, and 6 h (Figure 10). Densitometry results show a significant decrease in the level of pro-MMP-9 in H_2O_2-treated NRAs at 4 h and 6 h but not at 2 h. Protein expression was normalized using β-actin. DME medium with H_2O represents the vehicle internal control for H_2O_2 treatment and did not significantly affect MMP-9 protein expression in NRAs. Western blot results demonstrated that H_2O_2-induced oxidative stress significantly reduced the amount of pro-MMP-9 with the greatest reduction occurring

with treatment of 1.0 µM for 4h and 2.0 µM 6 h. A decrease in MMP-9 protein was unexpected given our previous result showing an increase in MMP-9 gene expression. Thus, I hypothesized this reduction in pro-MMP-9 was a result of cleavage to the parent resulting in a truncated active MMP-9. Other potential hypotheses include: gene expression had increased but not sufficient time had passed to increase protein expression in 6 h, another factor within the cell stopped translation of MMP-9 protein from increased mRNA expression, and H_2O_2-induced oxidative stress could increase the levels of endogenous inhibitors of MMP-9 such as TIMP-1 which could be sequestering MMP-9 as quickly as increase gene expression is producing MMP-9.

3.2.3 H_2O_2 - induced oxidative stress increases MMP-9 activity in astrocyte conditioned media.

To show that this was in fact occurring, gelatin zymography was performed on the conditioned media of NRA astrocytes. However, under our zymography conditions the level of MMP-9 activity was not conclusive (Figure 11). The conditioned media were then tested on a more sensitive MMP-9 activity assay, to measure the activity of MMP-9. This result showed a significant increase in active MMP-9 in the media of 0.5 µM H_2O_2 treated NRA cells at 2 h (Figure 12). In combination, PCR, Western Blotting and activity assays show that MMP-9 expression was being significantly affected by H_2O_2 treatment.

A)

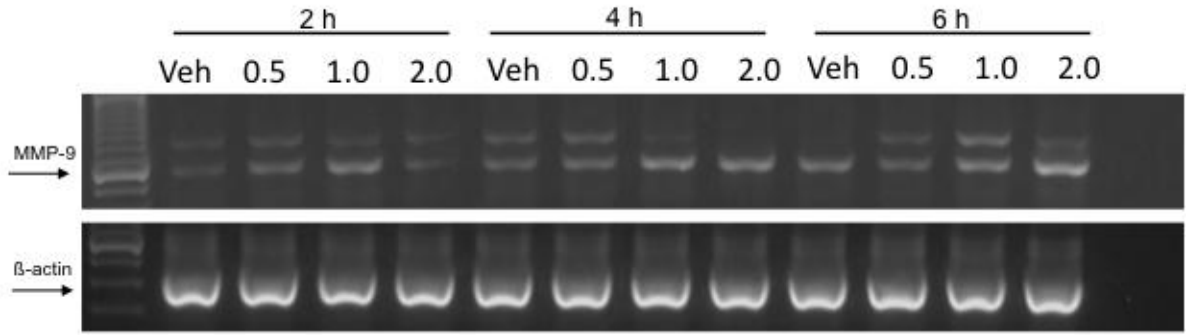

B)

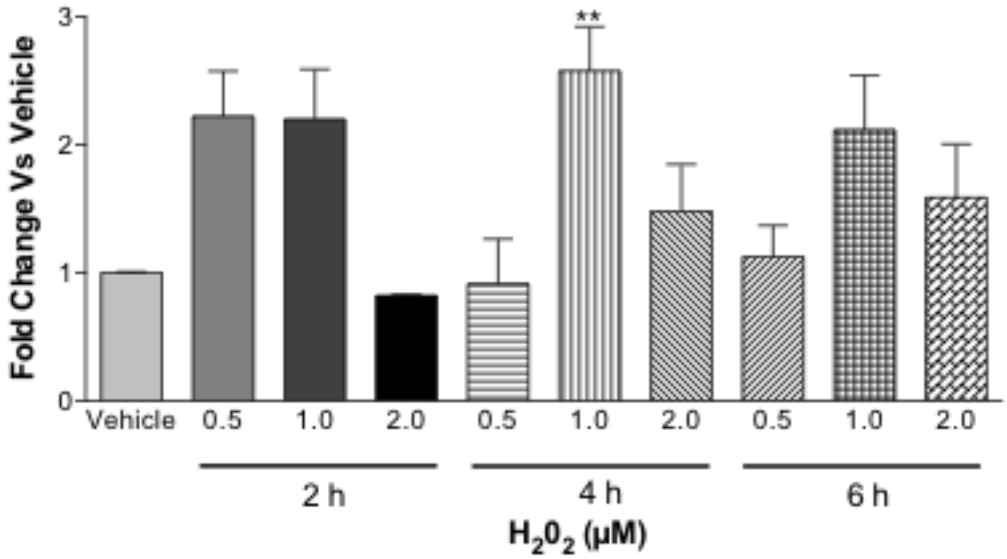

Figure 8: RT-PCR to detect the effect of H_2O_2 on MMP-9 gene expression in astrocytes (NRA).

Panel A) RT-PCR shows MMP-9 gene expression in NRA cells following treatment with vehicle and H_2O_2 0.5 , 1.0, and 2.0 µM for 2, 4, and 6 h. **Panel B)** Densitometry analysis shows MMP-9 expression is significantly higher in 1.0 µM H_2O_2-treated cells at 4 h compared to vehicle at 4h (N=3, two-way ANOVA with Bonferroni's post-test, interaction $F_{6,24}$=2.77, *p<0.05, H_2O_2 treatment $F_{3,24}$=10.50,*** p<0.0001 and time $F_{2,24}$=0.1241, p>0.05). β-actin was used as an internal control. NTC: negative control for RT-PCR.

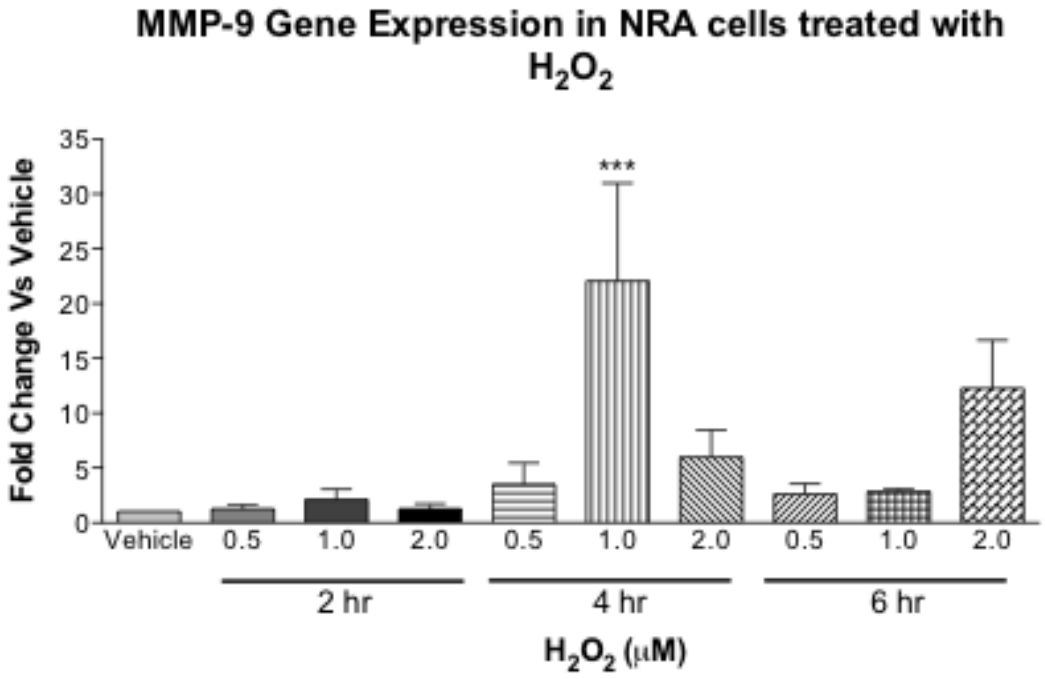

Figure 9: Quantitative-PCR (qPCR) to confirm MMP-9 gene expression in astrocytes (NRA).

MMP-9 gene expression in NRA cells following treatment with H_2O_2 for 2, 4, and 6 h. Statistical analysis shows MMP-9 expression is significantly higher in H_2O_2 -treated cells at 4 h with 1.0 µM and 6 h with 2.0 µM compared to vehicle (N=3, two-way ANOVA with Bonferroni's post-test, interaction $F_{6,24}$=4.12, *p<0.05, H_2O_2 treatment $F_{3,24}$=4.37, *p<0.05 and time $F_{2,24}$=4.89, *p<0.05). β-actin was used as an internal control.

A)

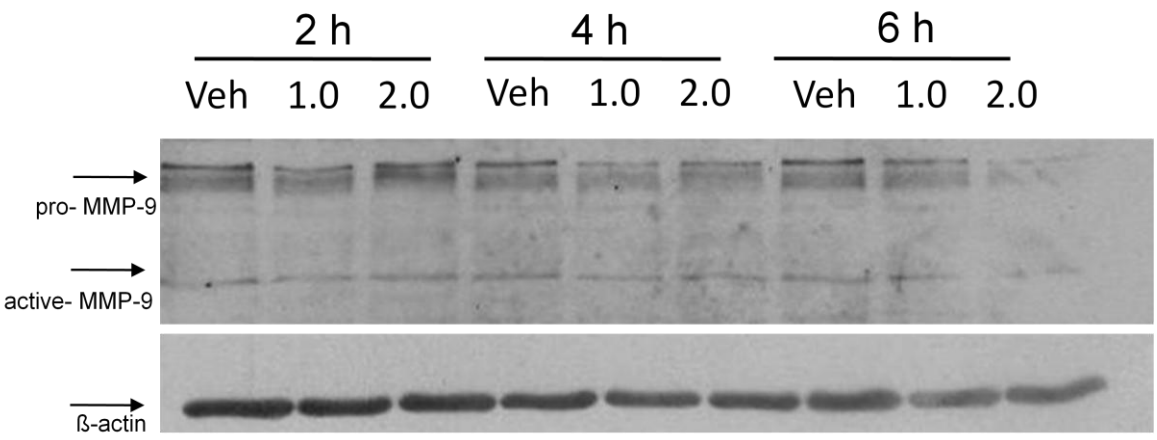

B)

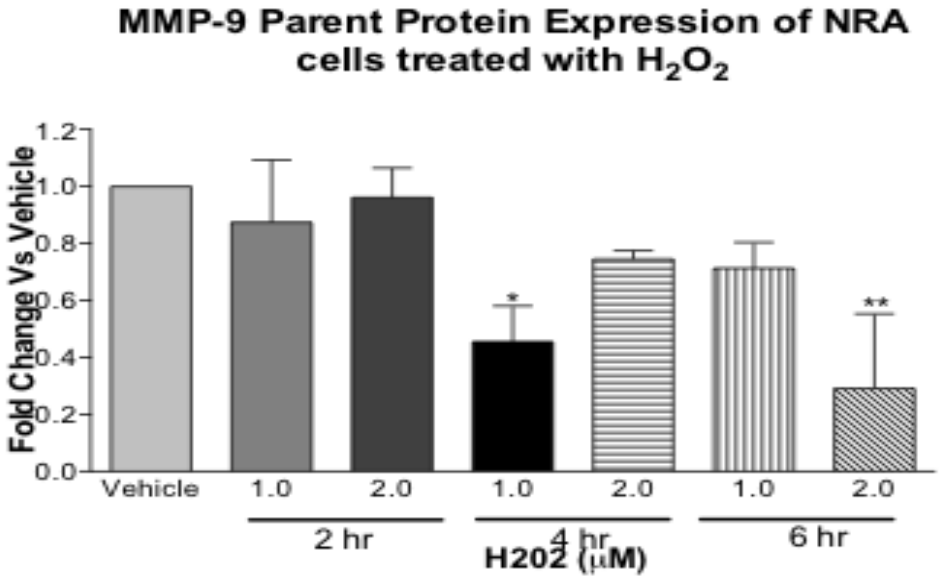

Figure 10: Western Blot to detect the effect of H_2O_2 on parent (pro-MMP-9) protein expression in astrocytes (NRA).

Panel A) Western blot shows MMP-9 protein expression in NRA cells following treatment with vehicle, 1µM H_2O_2, and 2µM H_2O_2 for 2, 4, and 6 h. **Panel B)** Densitometry analysis shows parent protein (pro-MMP-9) expression is significantly lower in H_2O_2 -treated cells than vehicle at 4 h 1.0 µM and 6 h 2.0 µM (N=3, two-way ANOVA, with Bonferroni's post-test, interaction $F_{4,18}$=2.915, $p>0.05$, H_2O_2treatment $F_{2,18}$=6.327,** $p<0.001$ and time $F_{2,18}$=3.706, *$p<0.05$). β-actin was used to normalize.

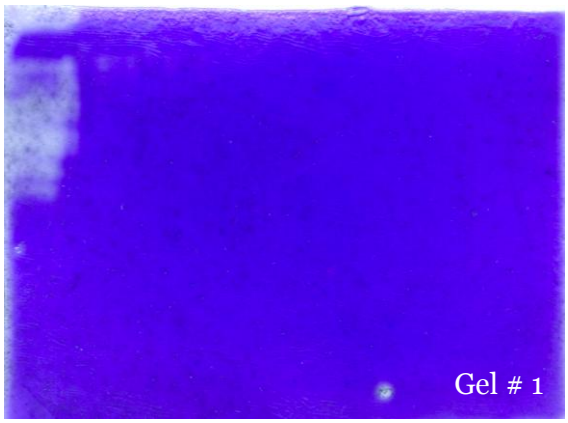

Figure 11: Zymograph to detect the effect of H_2O_2 on MMP-9 activity in astrocyte (NRA) conditioned media.

Conditioned media were collected from NRA cells treated with vehicle (lanes #1, 3, and 5) or H_2O_2 at 1.0 µM (lanes # 2, 4, and 6) for 4 h for analysis by zymography. MMP-9 activity was minimally detectable by this assay making the result inconclusive (N=3)

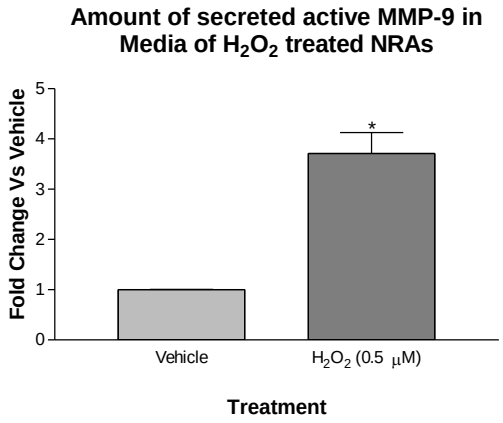

Figure 12: MMP activity assay to determine the effect of H_2O_2 treatment on MMP-9 activity in astrocyte (NRA) conditioned media.

Conditioned media collected from NRA cells treated with vehicle and H_2O_2 at 0.5 µM in 1% FBS for 30 min followed by a medium switch for 1.5 h. MMP activity is measured as amount of cleaved fluorescent peptide compared to vehicle (N=3, *t*-test, *$p<0.001$).

3.2.4 Immunofluorescence of MMP-9 to detect cellular response to H_2O_2-induced oxidative stress

To further understand the expression of MMP-9 in NRA cells after H_2O_2-induced oxidative stress, immunofluorescence (immunocytochemistry) was performed. NRA cells were treated with 1.0 μM H_2O_2 for 4 h to detect total MMP-9 (Figure 13). Immunofluorescence with MMP-9 antibody and Hoechst 33342 staining (nucleus) revealed a greater presence of MMP-9 in NRA cells treated with H_2O_2 treatment than H_2O alone. This result shows an overall increase in MMP-9 in cells treated with H_2O_2. These results provide further insight into what was happening to MMP-9 when the results of PCR, western blot and MMP activity assays were considered as a whole picture that H_2O_2-induced oxidative stress results in an overall increase in MMP-9 expression in astrocytes. However, it must be noted that it is complicated to understand the levels of MMP-9 expression when there are cleaved and active forms of a particular protein of interest.

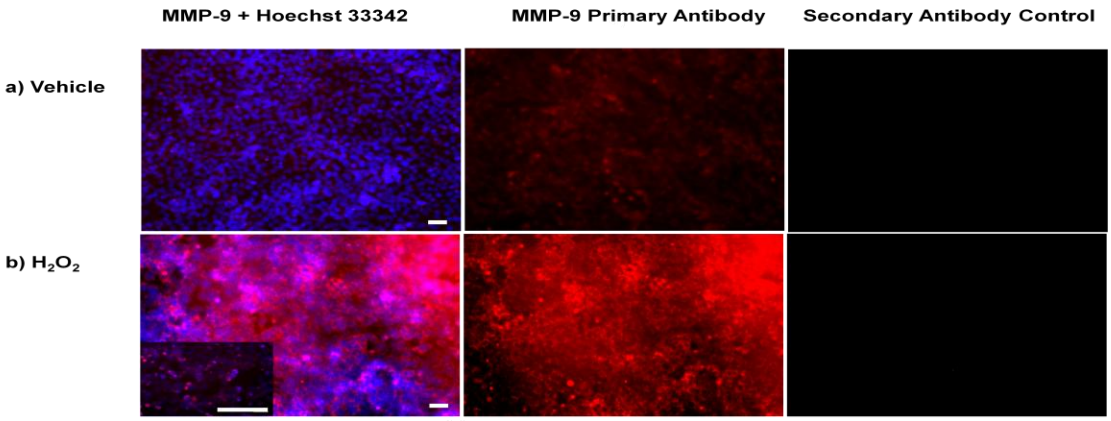

Figure 13: Immunoflourescence to detect the effect of H_2O_2 on the levels of MMP-9 protein in NRA cells.

NRA cells were treated with 1.0 μM H_2O_2 for 4 h to detect total MMP-9. Immunofluorescence with MMP-9 antibody and Hoechst 33342 staining (nucleus) revealed a greater presence of MMP-9 in NRA cells treated with H_2O_2 treatment than H_2O alone (N=3, images are representative). Secondary antibody control was done to detect non-specific binding. Images were captured at 10X magnification, higher power insert 20X magnification. Scale bars represent 50 microns.

3.3 H_2O_2-induced oxidative stress activates MAPK signaling pathways

To determine if mitogen-activated protein kinase (MAPK) signaling cascade could potentially be involved in oxidative stress-induced MMP-9 expression in astrocytes, H_2O_2 treatment was repeated to detect the activation of the signaling proteins (phosphorylation) on MAPK pathways by western blot. Treatment of NRA cells with H_2O_2 at 0.5, 1.0, and 2.0 µM for 2, 4, and 6 h induced a significant increase in the phosphorylation of p38 kinase (Figure 14) and c-Jun (Figure 15). Phosphorylation of p38 kinase increased in a dose- and time-dependent manner, phosphorylation increased with concentration of H_2O_2 and length of treatment. Phosphorylation of c-Jun at Serine 63 and Serine 73 increased with concentration of H_2O_2 but levels peaked during time point of 4 h. Total levels of c-Jun protein did not change significantly with treatment of H_2O_2; however at 4 h time point the levels did trend upwards. In contrast, treatment of NRA cells with H_2O_2 at 1.0 and 2.0 µM for 2, 4, and 6 h induced a minimal change in phosphorylation of extracellular signal-regulated kinases 1/2 (ERK1/2) (Figure 16). All phosphorylation levels were normalized using β-actin. DME medium with H_2O represents the vehicle internal control for H_2O_2 treatment and did not significantly affect phosphorylation levels of MAP kinase proteins in NRAs. The phosphorylation data suggests that the MAP kinase signaling pathways p38 and JNK may be highly involved in signaling during oxidative stress in NRA cells. By comparison, the ERK pathway may not be playing as important of a role, but we chose to continue the experiments with ERK to determine in order to demonstrate the effect of all three MAPK on MMP-9. The MAP kinase phosphorylation profiles with H_2O_2 treatment are in line with previous research that suggests reactive oxygen species can activate the

JNK, p38, and ERK pathways. Generally environmental stressors activate JNK and p38 kinases whereas growth factors and tumor promoters activate ERK1/2 (Simon *et al.* 2001). The MAPK phosphorylation results provide the insight that p38, JNK, and ERK1/2 known activators of AP-1, could potentially be upstream regulators of MMP-9 expression.

A)

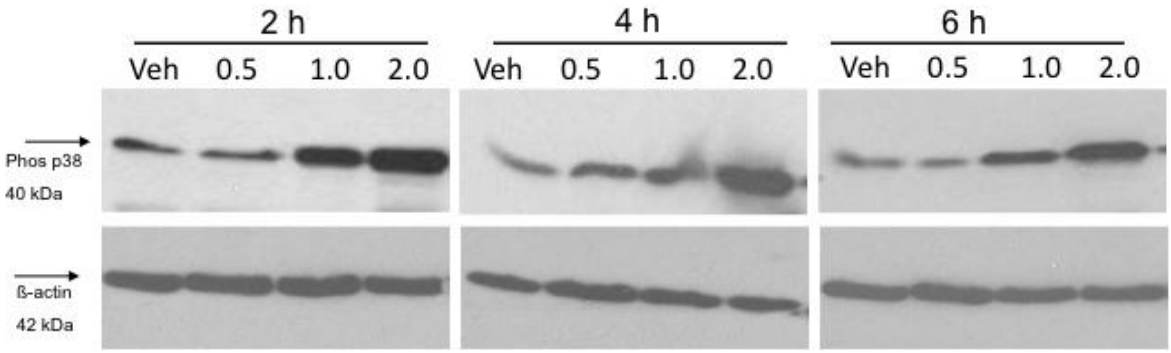

B)

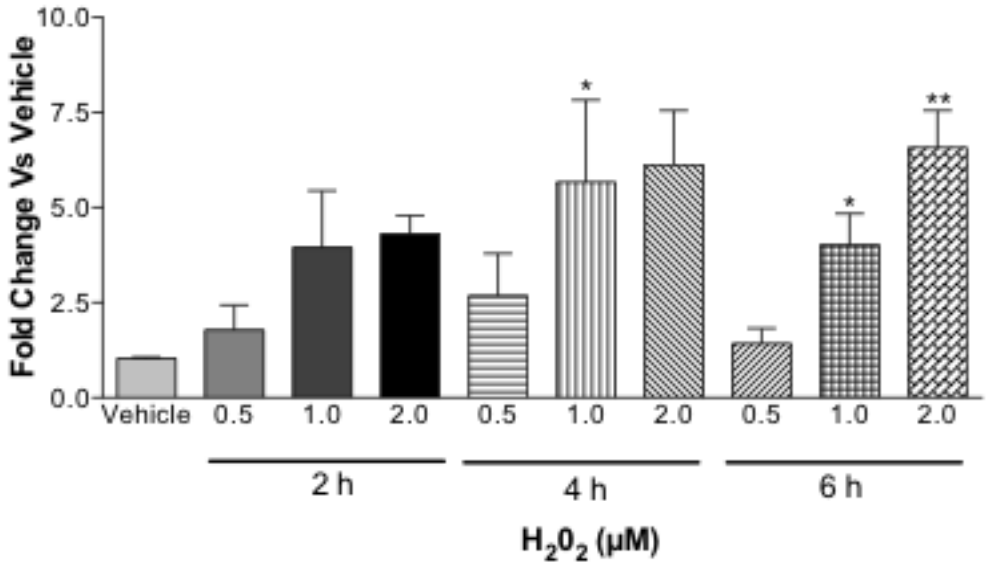

Figure 14: Western Blot to detect phosphorylation of p38 kinase in astrocytes (NRA) in response to H_2O_2- induced oxidative stress.

Panel A) Western blot shows the level of phosphorylated p38 kinase in NRA cells following treatment with H_2O_2 for 2, 4, and 6 h. Panel B) Densitometry analysis shows phosphorylated p38 is significantly greater in H_2O_2 -treated cells 2.0 µM at 2 h, 1.0 and 2.0 µM at 4 h and 1.0 and 2.0 µM at 6 h compared to vehicle (N=3, Two-way ANOVA with Bonferroni's post-test, Interaction $F_{6,24}$ = 0.4979, $p>0.05$; H_2O_2 treatment $F_{3,24}$=13.31, *$p<0.05$, **$p<0.01$; Time $F_{2,24}$=1.163, $p>0.05$). ß-actin was used to normalize.

A)

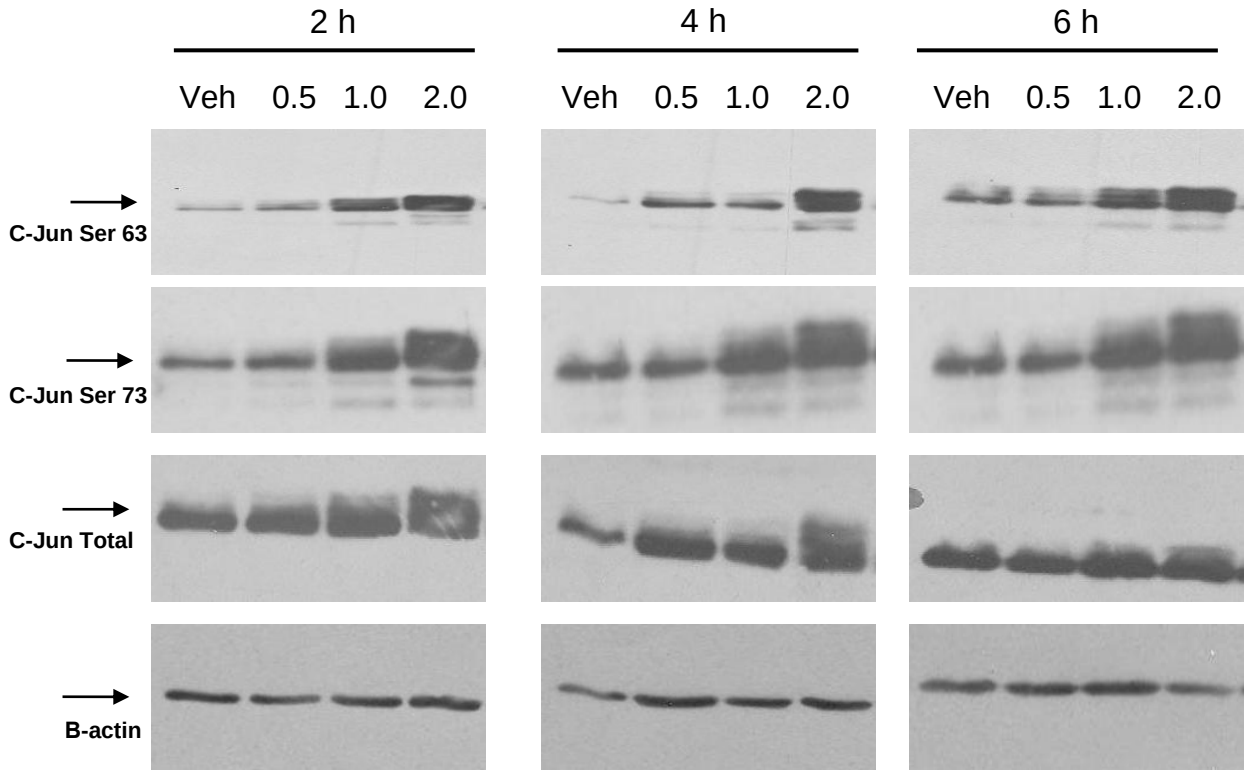
2 h
4 h
6 h
Veh 0.5 1.0 2.0
Veh 0.5 1.0 2.0
Veh 0.5 1.0 2.0
C-Jun Ser 63
C-Jun Ser 73
C-Jun Total
B-actin

B)

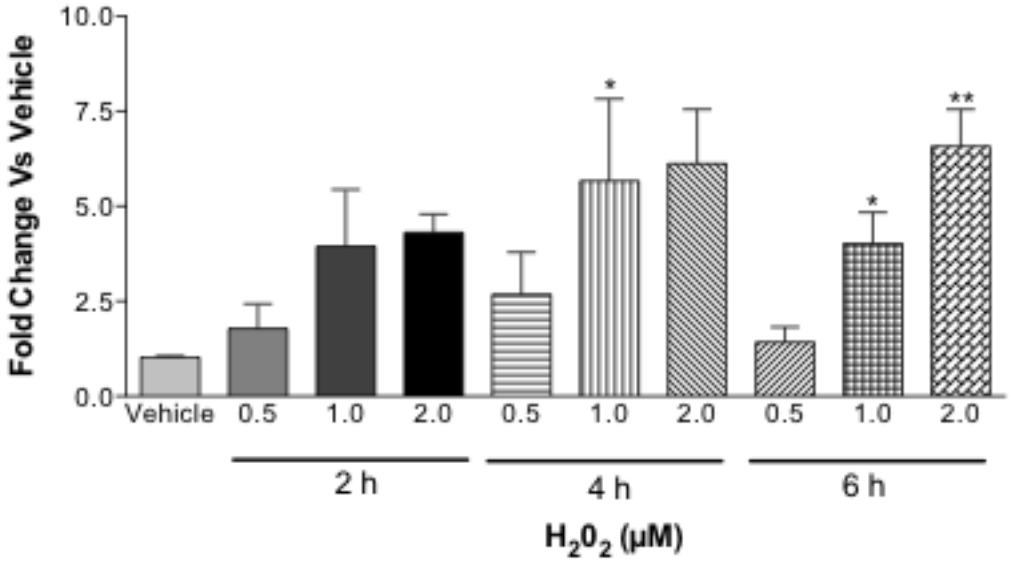
Fold Change Vs Vehicle
10.0
7.5
5.0
2.5
0.0
Vehicle 0.5 1.0 2.0 0.5 1.0 2.0 0.5 1.0 2.0
2 h
4 h
6 h
H_2O_2 (μM)

C)

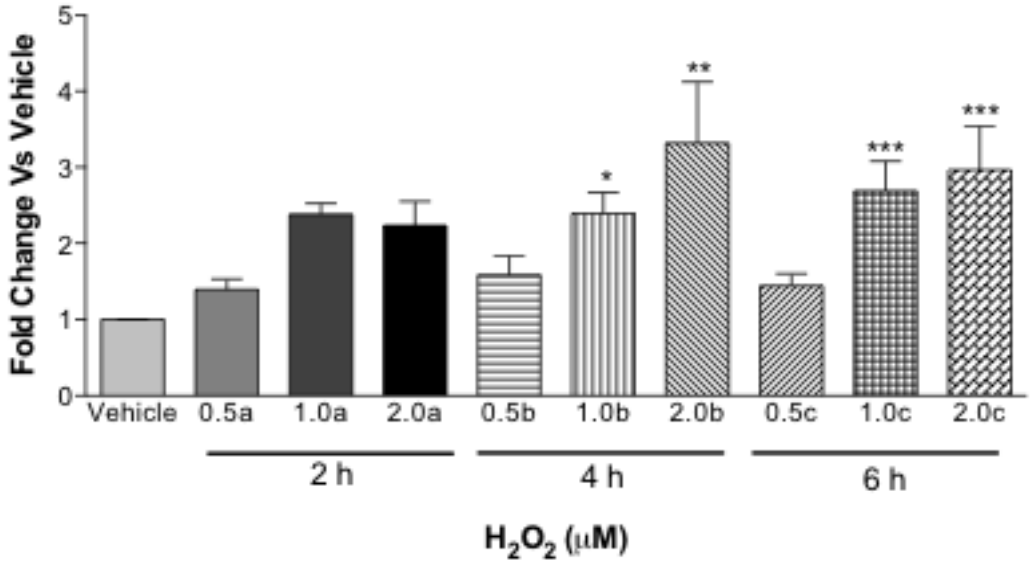
Fold Change Vs Vehicle
0
1
2
3
4
5
*
**
***
***
Vehicle
0.5a
1.0a
2.0a
0.5b
1.0b
2.0b
0.5c
1.0c
2.0c
2 h
4 h
6 h
H2O2 (μM)

D)

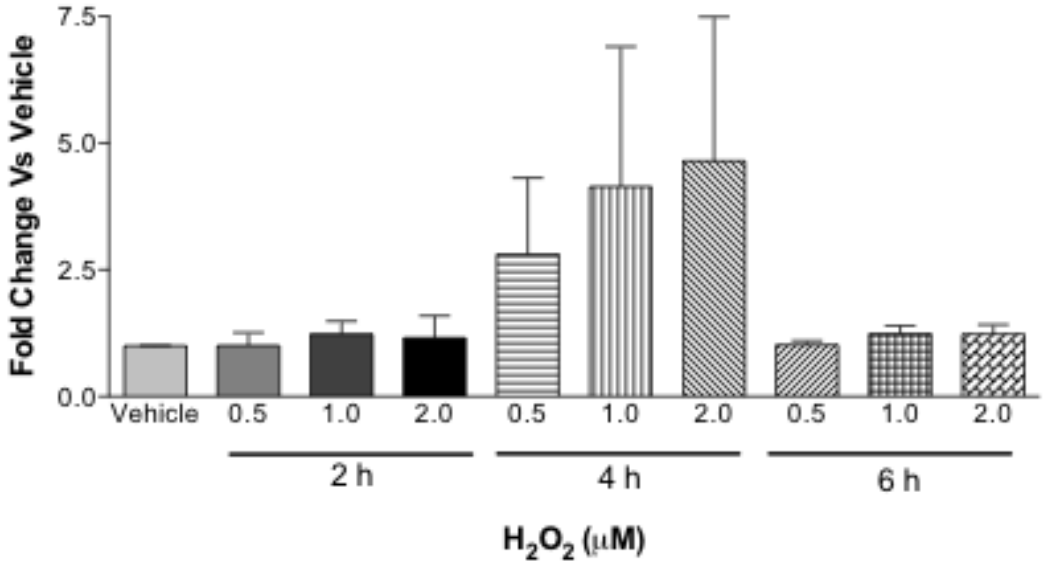
Fold Change Vs Vehicle
0.0
2.5
5.0
7.5
Vehicle
0.5
1.0
2.0
0.5
1.0
2.0
0.5
1.0
2.0
2 h
4 h
6 h
H2O2 (μM)

Figure 15: Western Blot to detect phosphorylation of c-Jun at Serine 63 and at Serine 73 and c-Jun total protein in astrocytes (NRA) in response to H_2O_2- induced oxidative stress.

Panel A) Western blot shows the level of phosphorylated c-Jun at Serine 63, the level of phosphorylated c-Jun at Serine 73 and the total c-Jun in NRA cells following treatment with Vehicle and H_2O_2 at 0.5, 1.0, and 2.0 μM for 2, 4, and 6 h. **Panel B)** Densitometry analysis shows the level of phosphorylated c-Jun at serine 63 is significantly greater in H_2O_2 -treated cells than vehicle at 4h (N=4, Two-way ANOVA with Bonferroni's post-test, Interaction $F_{6,33}$=0.5704, $p>0.05$; H_2O_2 treatment, $F_{3,33}$=7.452,* *$p<0.05$, * $p<0.001$; Time $F_{2,33}$=1.409, $p>0.05$). β-actin was used to normalize.

Panel C) Densitometry analysis shows phosphorylated c-Jun at serine 73 is significantly greater in H_2O_2 -treated cells than vehicle at 2h, 4h and 6h (N=3, Two-way ANOVA with Bonferroni's post-test, Interaction $F_{6,36}$=0.6247, $p>0.05$; H_2O_2 treatment $F_{3,36}$=18.38, *$p<0.05$, **$p<0.01$, ***$p<0.001$; Time $F_{2,33}$=1.409, $p>0.05$). β-actin was used to normalize.

Panel D) Densitometry analysis shows no significant difference in total c-Jun in H_2O_2 -treated cells than vehicle (N=4, Two-way ANOVA with Bonferroni's post-test $p>0.05$). β-actin was used to normalize.

A)

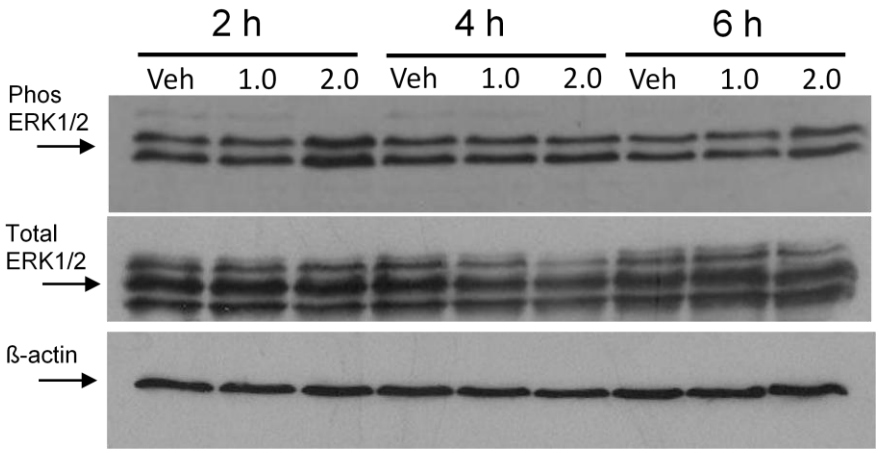
2 h
4 h
6 h
Veh
1.0
2.0
Veh
1.0
2.0
Veh
1.0
2.0
Phos ERK1/2
Total ERK1/2
ß-actin

B)

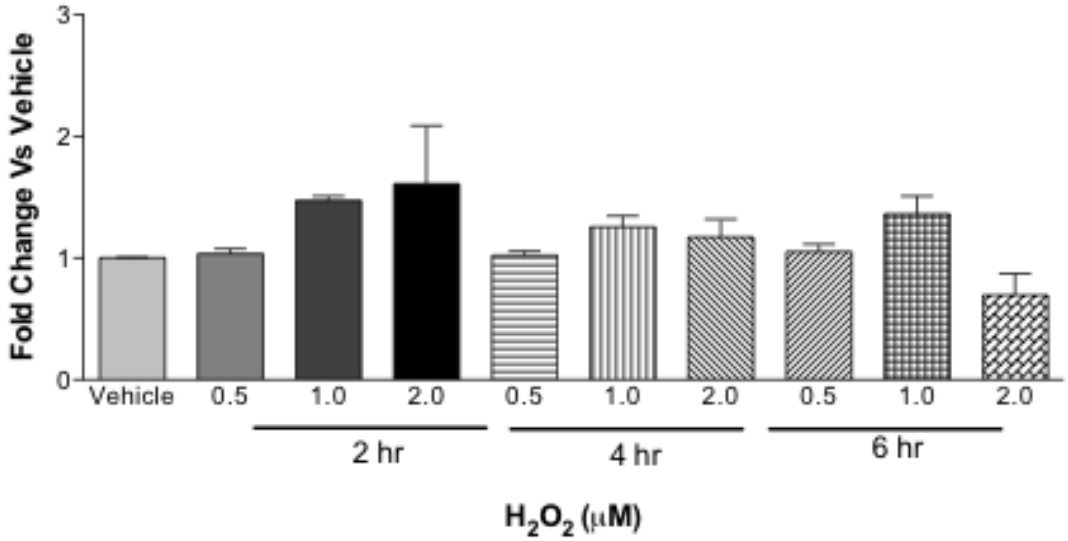
Fold Change Vs Vehicle
0
1
2
3
Vehicle
0.5
1.0
2.0
0.5
1.0
2.0
0.5
1.0
2.0
2 hr
4 hr
6 hr
H2O2 (μM)

C)

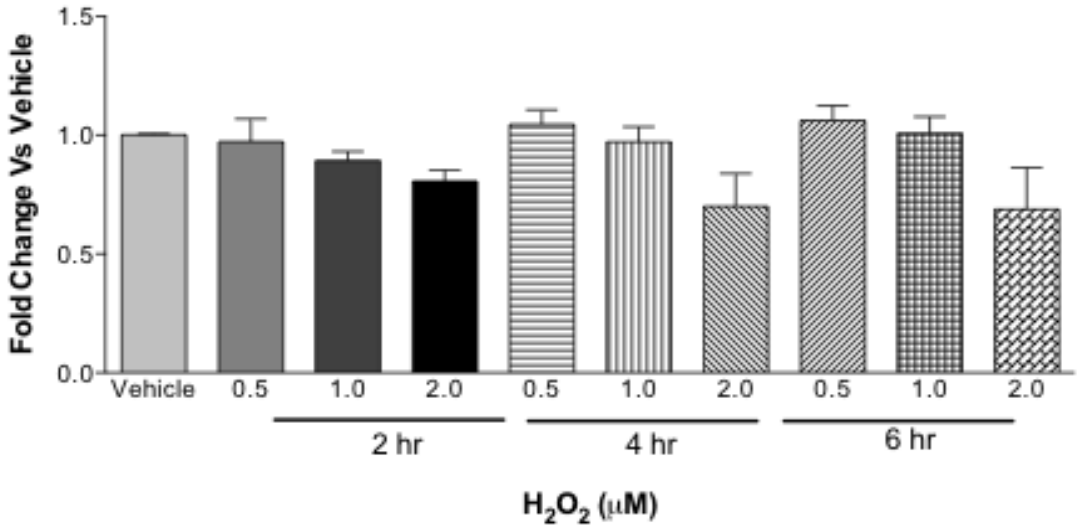

Figure 16: Western Blot to detect the phosphorylation of ERK1/2 kinases and total ERK1/2 kinases in astrocytes (NRA) in response to H_2O_2- induced oxidative stress. **Panel A)** Western blot shows phosphorylated ERK1/2 in NRA cells following treatment with Vehicle and H_2O_2 at 1.0, and 2.0 μM for 2, 4, and 6 h. **Panel B)** Densitometry analysis shows phosphorylated ERK1/2 does not change significantly in H_2O_2 -treated cells compared to vehicle (N=3, two-way ANOVA with Bonferroni's post-test $p>0.05$). β-actin was used to normalize. **Panel C)** Densitometry analysis shows total of ERK1/2 expression is not significantly different in H_2O_2 -treated cells than control (N=3, two-way ANOVA with Bonferroni's post-test $p>0.05$). β-actin was used to normalize.

3.4 Characterization of the roles of MAPK Signaling Pathways in regulation of MMP-9 Expression

3.4.1 H_2O_2-induced MMP-9 gene expression is mediated through MAPK signaling pathway in astrocytes

Results of phosphorylation of MAP kinases by western blot suggested a potential role of MAP kinases in regulation of MMP-9 expression. To determine if MAP kinases were playing a role in regulation of MMP-9 expression, the levels of MMP-9 mRNA, protein and MMP-9 activity were studied in the presence of chemical inhibitors specific to JNK, p38 and ERK1/2. To determine if the inhibitors of MAP kinases could reduce mRNA levels of MMP-9, the time points of H_2O_2 treatment from my preliminary experiments (Figure 8, Figure 9) that yielded greatest increase (1.0 μM for 4 h) were used. NRA cells pretreated for 30 min with chemical inhibitors for p38, JNK, and ERK1/2 at 10 and 20 μM showed a significant reduction in MMP-9 mRNA levels by quantitative RT-PCR (Figure 17). This result suggests that in NRA cells the MAP kinase signaling pathways are involved in up-regulation of MMP-9 expression following H_2O_2-induced oxidative stress.

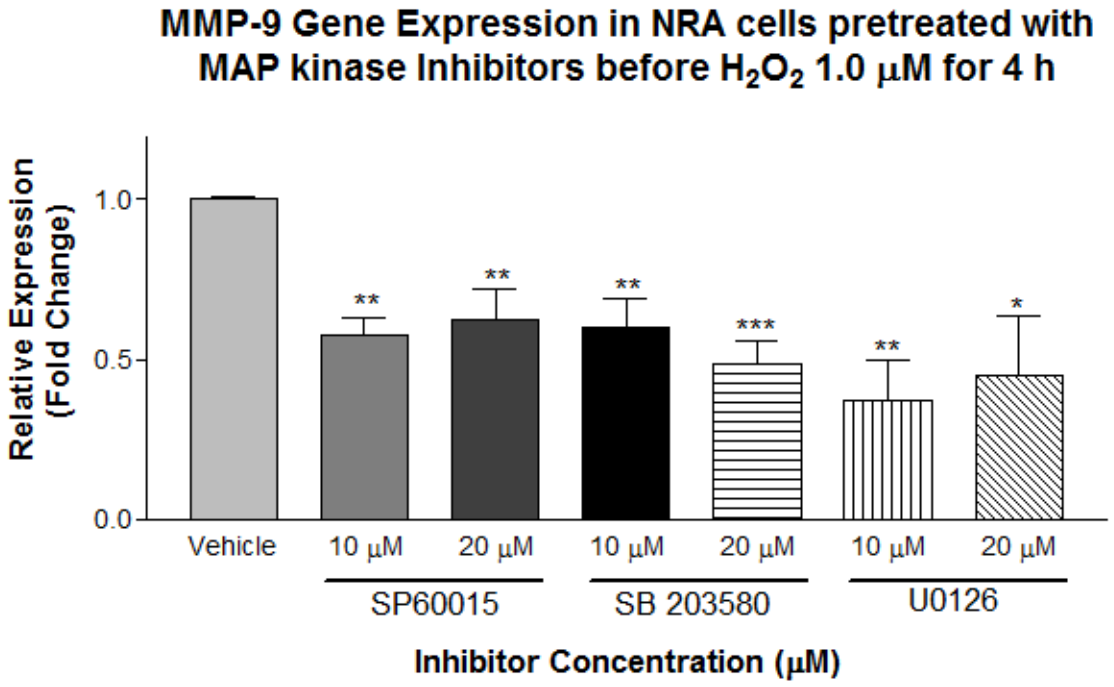

Figure 17: RT-qPCR for MMP-9 gene expression in astrocytes (NRA) in the presence of MAPK inhibitors.

NRA cells pretreated with MAP Kinase Inhibitor SP60015 (JNK Inhibitor), SB 203580 (p38 Inhibitor) and U0126 (ERK1/2 Inhibitor) for 30 min at 10 and 20 μM before treating with H_2O_2 at 1.0 μM for 4 h. Treatment with MAP kinase inhibitors reduced the relative expression of MMP-9 by real-time quantitative compared to vehicle (N=3, two-way ANOVA with Bonferroni's post-test, Interaction $F_{3,16}$=0.3538, $p>0.05$; MAPK Inhibitor $F_{3,16}$=13.52, *$p<0.05$,**$p<0.01$,***$p<0.001$; Concentration $F_{1,16}$ =0.00052, $p>0.05$). β-actin was used to normalize.

3.4.2 H_2O_2-Induced MMP-9 protein expression is mediated through MAPK Signaling Pathway in Astrocytes

Western blotting was done for pro-MMP-9 (parent protein) and cleaved MMP-9 (active form) treated with 1.0 µM for 4 and 6 h. The vehicle controls demonstrated that H_2O_2-induced oxidative stress decreased the amount of parent protein but increased the amount of cleaved active MMP-9 protein. This further validates my previous result that although parent protein was reduced due to cleavage, the cleaved amount of MMP-9 was increased (Figure 18). Treatment with JNK, p38 and ERK inhibitor (20 µM) further reduced the amount of pro-MMP-9 parent protein at 6 h without significant effect on cleaved MMP-9 active protein (Figure 19). The effectiveness of chemical inhibitors was confirmed (n=1) by western blot to show that phosphorylation of MAP kinases was in fact reduced in these treatments (data not shown). Together, these results demonstrate that the MAP kinase signaling cascade plays a role in the regulation of MMP-9 expression. Gene and protein expression data demonstrates that inhibition of MMP-9 expression is achieved by blocking MAP kinase signaling pathways.

A)

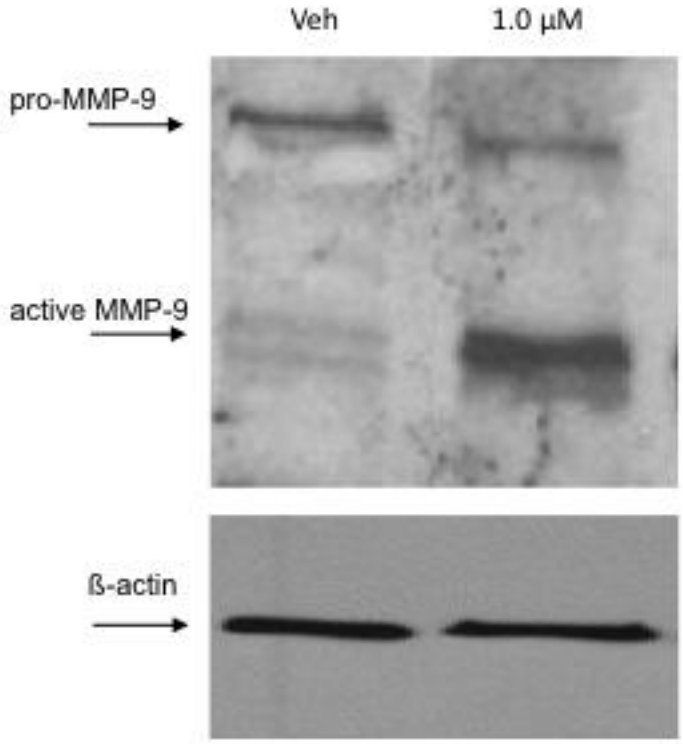
Veh
1.0 µM
pro-MMP-9
active MMP-9
ß-actin

B)

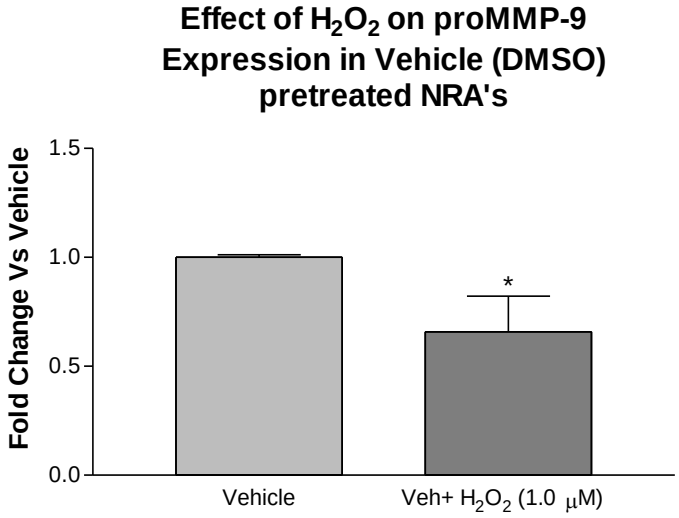
Effect of H_2O_2 on proMMP-9 Expression in Vehicle (DMSO) pretreated NRA's
Fold Change Vs Vehicle
1.5
1.0
0.5
0.0
*
Vehicle
Veh+ H_2O_2 (1.0 µM)

C)

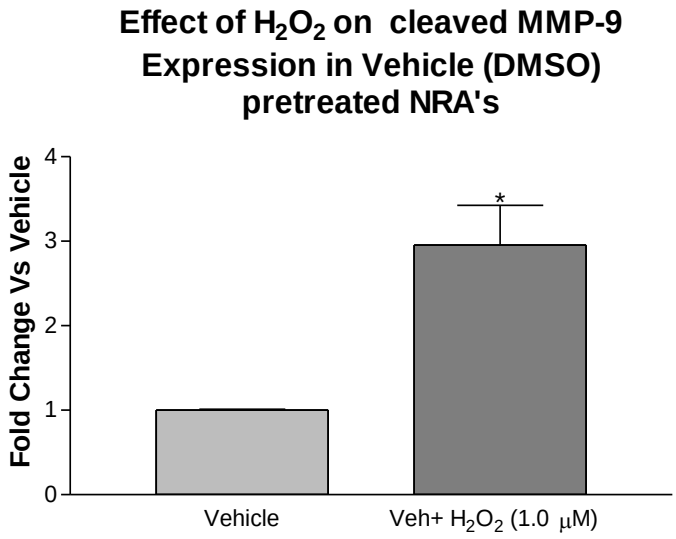

Figure 18: Western blot to detect the levels of pro-MMP-9 (parent protein) and cleaved MMP-9 in astrocytes (NRA) treated with H_2O_2 in presence of 0.1% DMSO.

Panel A) Western blot for NRA cells pretreated with 0.1% DMSO for 30 min before treating with vehicle -H_2O or H_2O_2 at 1.0 μM for 6 h. **Panel B)** Densitometry analysis shows pro-MMP-9 (parent protein) expression was not affected by the presence of 0.1% DMSO and was significantly lower in H_2O_2 -treated cells than vehicle at 6 h (N=3, *t* test, *p<0.05). β-actin was used to normalize. **Panel C)** Densitometry analysis shows cleaved form of MMP-9 expression was significantly higher in H_2O_2 -treated cells than vehicle at 6 h (N=3, *t* test , *p<0.05). β-actin was used to normalize.

A)

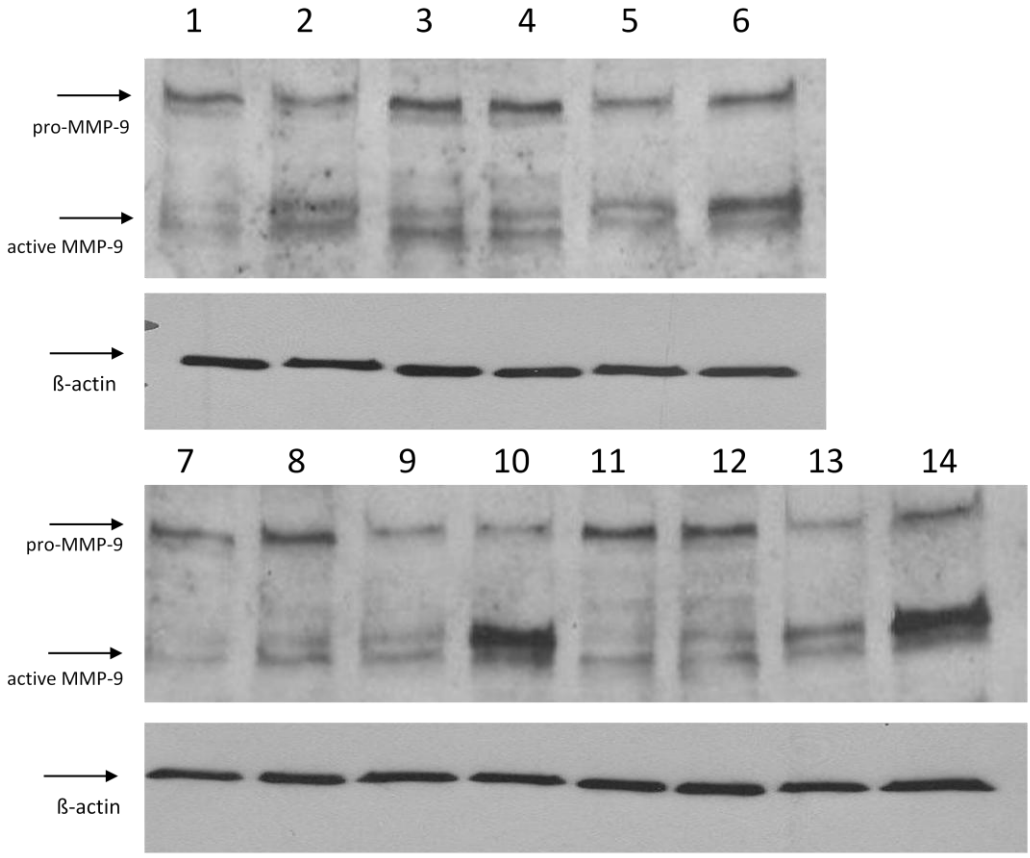

Lane	Treatment
1	Vehicle (0.1% DMSO) - H_20
2	Vehicle (0.1% DMSO) - H_20_2 1.0 µM
3	JNK Inhibitor 20 µM - H_20
4	JNK Inhibitor 10 µM - H_20
5	JNK Inhibitor 20 µM - H_20_2 1.0 µM
6	JNK Inhibitor 10 µM - H_20_2 1.0 µM
7	p38 Inhibitor 20 µM - H_20
8	p38 Inhibitor 10 µM - H_20
9	p38 Inhibitor 20 µM - H_20_2 1.0 µM
10	p38 Inhibitor 10 µM - H_20_2 1.0 µM
11	ERK Inhibitor 20 µM - H_20
12	ERK Inhibitor 10 µM - H_20
13	ERK Inhibitor 20 µM - $H_20_2$1.0 µM
14	ERK Inhibitor 10 µM - H_20_2 1.0 µM

B)

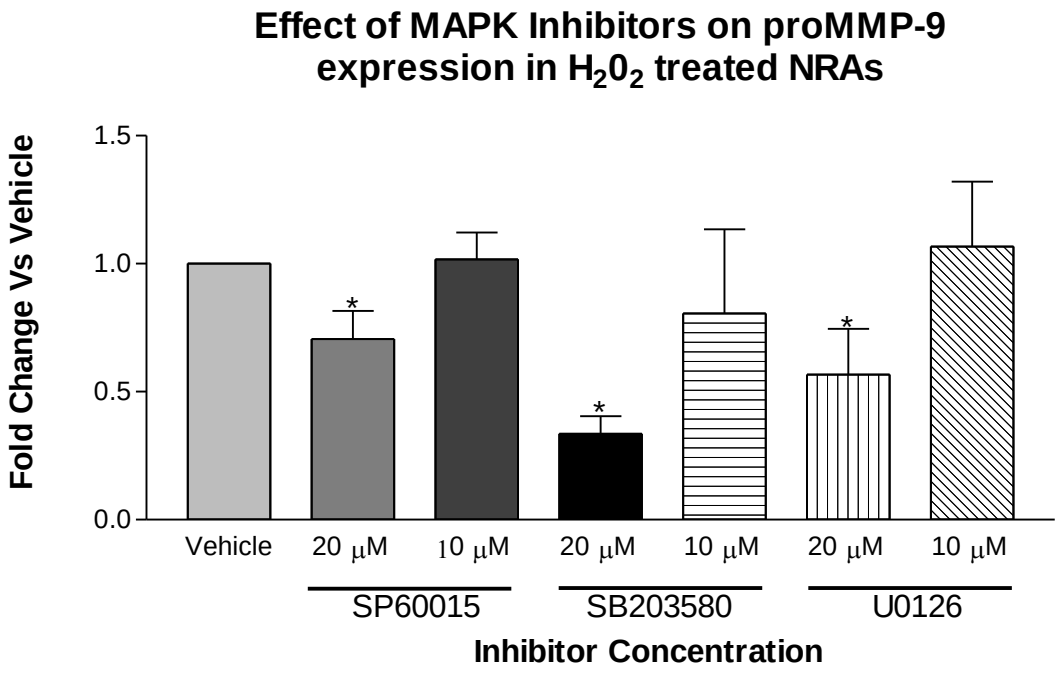
Effect of MAPK Inhibitors on proMMP-9 expression in H_20_2 treated NRAs
Fold Change Vs Vehicle
1.5
1.0
0.5
0.0
*
*
*
Vehicle
20 μM
10 μM
20 μM
10 μM
20 μM
10 μM
SP60015
SB203580
U0126
Inhibitor Concentration

C)

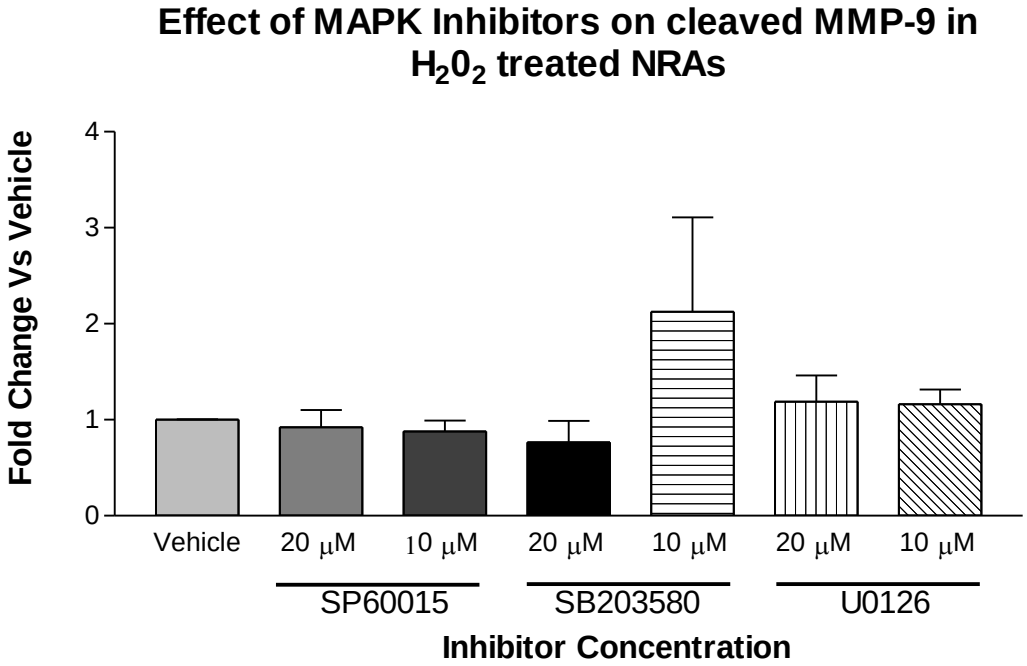
Effect of MAPK Inhibitors on cleaved MMP-9 in H_20_2 treated NRAs
Fold Change Vs Vehicle
4
3
2
1
0
Vehicle
20 μM
10 μM
20 μM
10 μM
20 μM
10 μM
SP60015
SB203580
U0126
Inhibitor Concentration

Figure 19: Western blot to detect the levels of pro-MMP-9 (parent protein) and cleaved MMP-9 in astrocytes (NRA) in the presence of MAPK inhibitors when treated with H_2O_2.

Panel A) Western blot shows NRA cells pretreated with MAP kinase inhibitor SP60015 (JNK Inhibitor), SB 203580 (p38 Inhibitor) and U0126 (ERK1/2 Inhibitor) for 30 min at 10 and 20 μM before treating with H_2O_2 at 1.0 μM for 6 h. **Panel B)** Densitometry analysis shows treatment with MAP kinase inhibitors 20 μM reduced the expression of pro-MMP-9 (parent protein) (92 kDa) compared to vehicle (N=3, one-way ANOVA with Dunnett's post test, $F_{3,8}$=6.519, *p<0.05). β-actin was used to normalize. **Panel C)** Densitometry analysis shows treatment with MAP kinase inhibitors had no significant effect on the levels of cleaved-MMP-9 compared to vehicle (N=3, one-way ANOVA, p>0.05).

3.4.3 Immunofluorescence to detect cellular response to MAPK inhibition of MMP-9 expression in H_2O_2 treated astrocytes.

To further understand the effect of MAP kinases on the expression of MMP-9 in NRA cells after H_2O_2-induced oxidative stress, immunofluorescence (immunocytochemistry) was performed. NRA cells were pre-treated with JNK, p38 and ERK inhibitor (20μM) for 30 min before treatment with 1.0 μM H_2O_2 for 4 h to detect the levels of cellular MMP-9 (Figure 20). Immunofluorescence with a MMP-9 antibody and Hoechst 33342 staining revealed a reduction of MMP-9 in NRA cells treated with the inhibitors + H_2O_2 treatment compared to controls. This result shows an overall decrease in MMP-9 in cells treated with JNK and p38 inhibitor + H_2O_2. This result with my previous PCR, western blot and MMP activity assay results suggests that JNK and p38 kinases play a significant role in the signaling of MMP-9 expression in H_2O_2-induced oxidative stress.

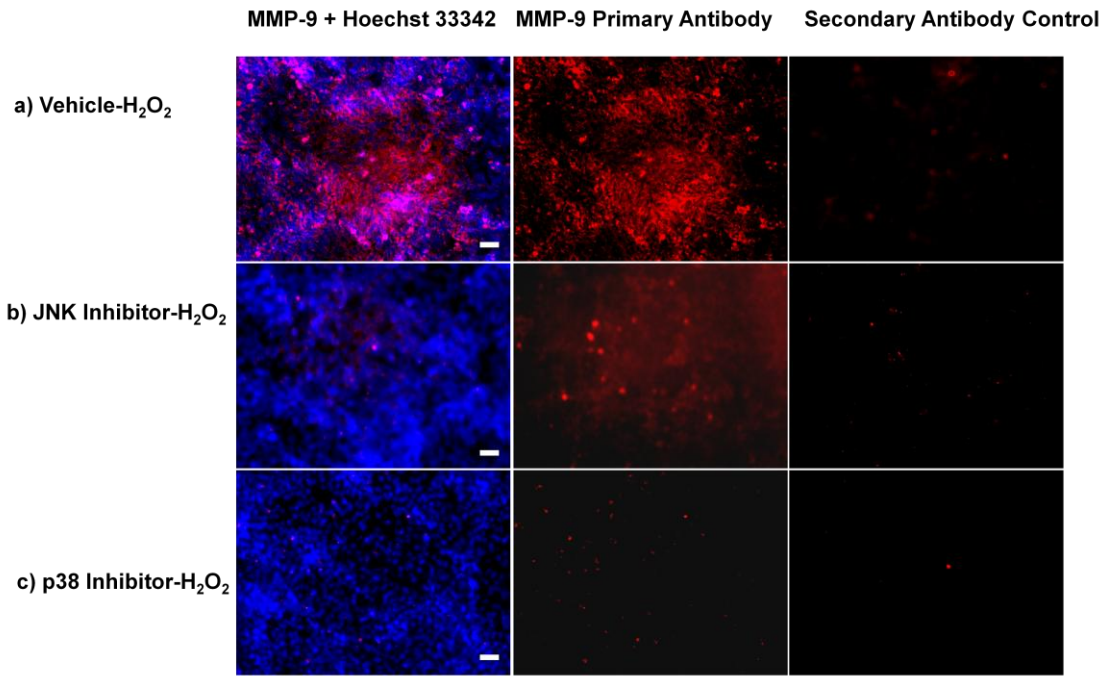

Figure 20: Immunofluorescence to detect the levels of MMP-9 protein in NRA cells pretreated with MAPK inhibitors.

Immunofluorescence shows MMP-9 protein in NRA cells pretreated with MAP kinase inhibitor SP60015 (JNK Inhibitor), SB 203580 (p38 Inhibitor) for 30 min at 20 µM before treating with H_2O_2 at 1.0 µM for 4 h. The images are: **a)** NRA cells treated with inhibitor vehicle and H_2O_2. **b)** NRA cells treated with SP60015 (JNK Inhibitor) and H_2O_2. **c)** NRA cells treated with SB 203580 (p38 Inhibitor) and H_2O_2. Secondary antibody control was done to detect non-specific binding. Images were captured at 10X magnification. Scale bar represents 50 microns.

3.4.4 Effect of MAPK Signaling Pathway on baseline expression of MMP-9

In order to decipher how the inhibitors may affect the expression of MMP-9, data collected was reanalyzed to determine the effect on baseline expression. This was of interest because of the lack of ERK phosphorylation from initial phosphorylation profiles, but the profound effect ERK inhibitors had on both gene and protein expression. These results did not demonstrate that any of the MAPK inhibitors were significantly effecting baseline expression (data not shown).

3.5. *MAPK Signaling Pathway Mediates MMP-9 Expression through Activator Protein 1 (AP-1)*

HEK293 cells were transiently transfected with pGL-3 reporter gene vector, which carries an insert from AP-1 binding site cloned from the promoter region of human MMP-9 gene. In addition, HEK293 cells were also transiently transfected with a commercial pTL-Luc reporter gene vector that contains multiple repeats of AP-1 binding site. The controls for the assay were the transfection of cells with empty pGL-3 or pTL vector without the AP-1 insert. After 48 h recovery post-transfection, the cells were treated in the presence of 20 μM MAPK inhibitors for 30 min followed by 1.0 μM H_2O_2 for 30 min. PMA was used as a positive control known to induce AP-1 activity in HEK293 cells (previous shown data Figure 6). Reporter gene assay was performed to show the effect of H_2O_2 on AP-1 induction and the MAPK inhibitors on reducing AP-1 induction, since AP-1 induction is directly proportional to luciferase activity. Data shows a significant AP-1 induction in H_2O_2 stimulated-HEK293 cells (Figure 21). This result indicates that H_2O_2-induced MMP-9 gene expression goes through the MAPK-AP1 pathway, suggesting that ROS activates the MAP kinases, and activated MAP kinases activate AP-1 which then turns on MMP-9 gene

expression. The MAPK inhibitors were not all able to reduce AP-1 reporter gene activity in the commercial AP-1 vector but all reduced the activity of AP-1 in the MMP-9 promoter vector (Figure 22). In addition, empty vector control showed that the AP-1 vectors were strongly stimulated by H_2O_2 treatment and had significantly greater reporter gene activity than their complimentary empty vector (Figure 23). It should be noted that HEK293 cells were chosen for transfection due to the extremely low transfection efficiency (<5%) of NRA cells previously determined in our laboratory (data not shown).

A)

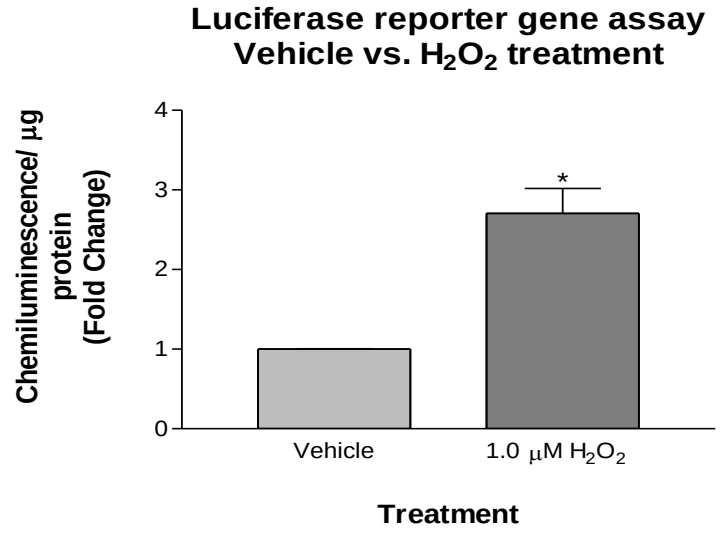

B)

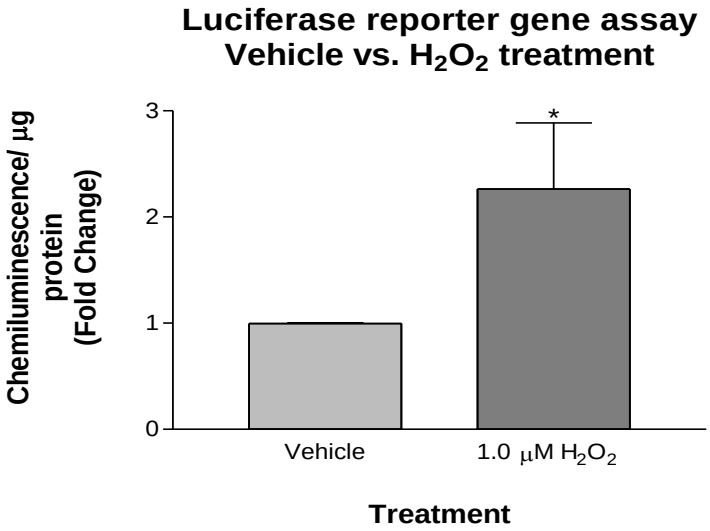

Figure 21: Reporter Gene Assay for the effect of H_2O_2 on AP-1 Transcriptional Activity.

HEK293 cells were transfected with pTL/AP-Luc vector **(Panel A)** and pGL-3/AP-1 **(Panel B)** vector and then treated with H_2O_2 at 1.0 µM for 30 min. H_2O_2 strongly stimulated reporter gene activity of pTL/AP-Luc plasmid at 30 min (N=3, *t*-test, *$p<0.05$). pGL-3/AP-1 plasmid showed the similar response at 30 min (N=3, t-test, one-tailed $p<0.05$).

A)

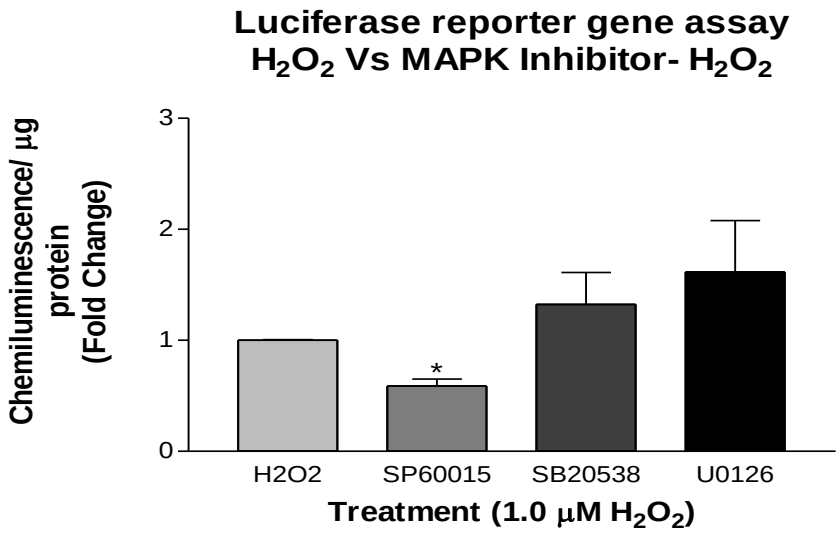

B)

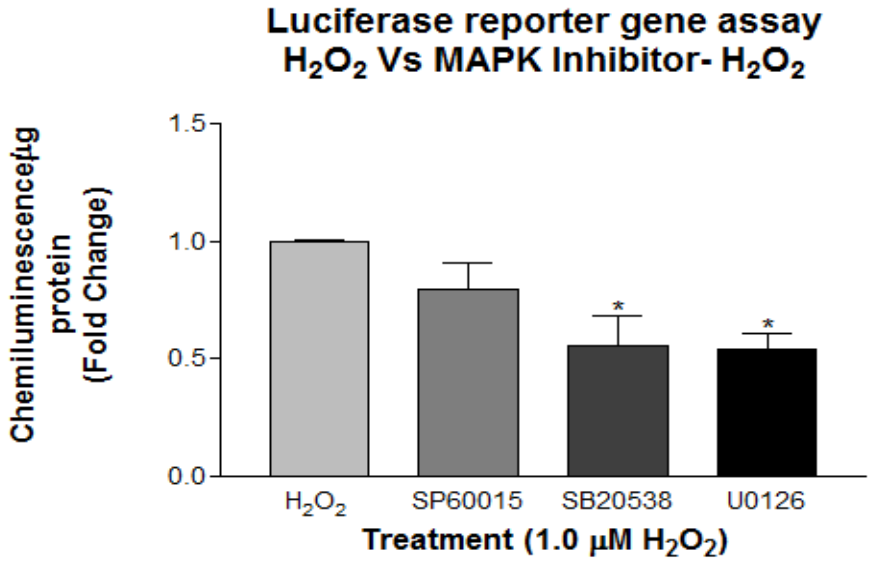

Figure 22: Reporter Gene Assay for the effect of H_2O_2 on AP-1 Transcriptional Activity in the presence of MAPK inhibitors.

HEK293 cells were transfected with pTL/AP-Luc vector **(Panel A)** or pGL-3/AP-1 vector **(Panel B)** and then pretreated with MAP kinase inhibitors, SP60015 (JNK inhibitor), SB 203580 (p38 inhibitor) or U0126 (ERK1/2 inhibitor) for 30 min at 20 µM before treatment with H_2O_2 at 1.0 µM for 30 min. Pretreatment with SP60015 (JNK inhibitor) in pTL/AP-Luc vector significantly reduced reporter gene activity (Panel A: N=3, One-way ANOVA, $p>0.05$, t-test, $*p<0.05$). Pretreatment with all MAPK inhibitors in pGL-3/AP-1 vector reduced reporter gene activity (Panel B: N=3, one-way ANOVA with Dunnett's post test $F_{3,8}=6.152$, $*p<0.05$).

A)

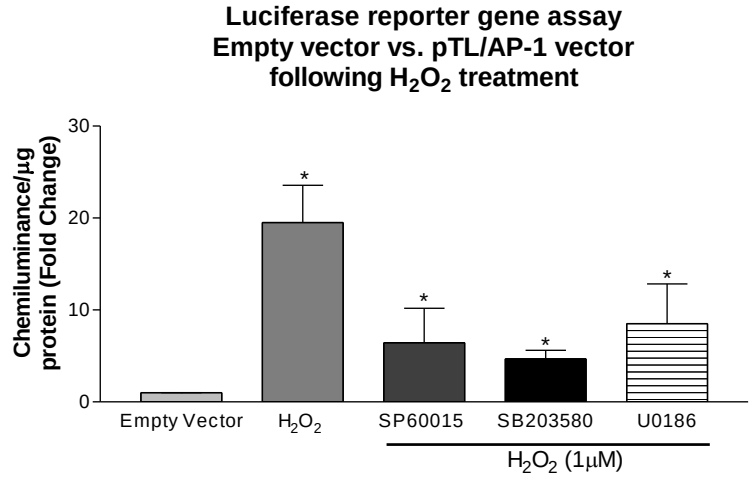

B)

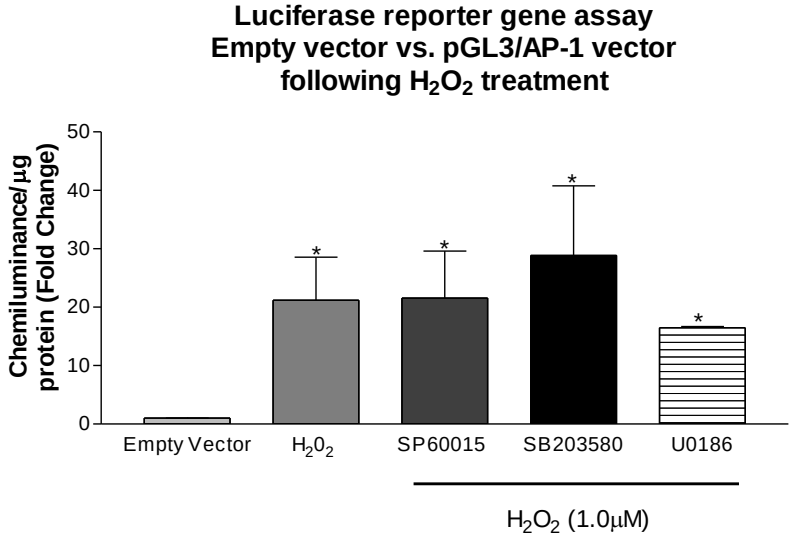

Figure 23: Luciferase reporter gene assay (empty vector controls).

HEK293 cells were transfected with either pTL/AP-Luc vector, pGL-3/AP-1 vector, empty pTL and empty pGL-3 vector and then pretreated with MAP kinase inhibitor SP60015 (JNK inhibitor), SB 203580 (p38 inhibitor) and U0126 (ERK1/2 inhibitor) for 30 min at 20 µM before treatment with H_2O_2 at 1.0 µM for 30 minutes. The AP-1 vectors were strongly stimulated by H_2O_2 treatment and has significantly greater reporter gene activity than their complimentary empty vector for AP-1/PTL (**Panel A**) (N=3, one-way ANOVA, $p<0.05$) for AP-1/pGL-3 (**Panel B**) (N=3, one-way ANOVA, $p>0.05$, t-test, *$p<0.05$).

3.6 Inhibition of MMP-9 expression may reduce the permeability of an in vitro model of the blood-brain barrier.

3.6.1 Permeability Testing (Pe Test)

An *in vitro* model of the BBB using SV-ARBEC (immortalized rat brain microvascular endothelial cells) cells was used to measure barrier permeability with the fluorescent dye marker sodium fluorescein. Initially, Pe test was used to ensure that the brain endothelial cells form a tight monolayer on the semi-permeable membrane of the culture inserts. The three wells with the cells were compared to three wells without cells to determine the permeability in a top-down direction of the cell layer. Pe test demonstrates that after 6 days in culture, the permeability coefficient of the *in vitro* BBB model was 0.56 X 10^{-3} cm/min for top to bottom transport (Figure 24, Panel A). The Pe value indicates that the BBB monolayer was tight and the permeability of the *in vitro* BBB model was low.

3.6.2 Effect of H_20_2 on the permeability of the in vitro BBB model

My hypothesis is founded on previous research that suggests ROS such as H_2O_2 is involved in the disruption of the BBB during cerebral ischemia or ischemic stroke. Thus, my goal was to replicate in the *in vitro* model whether H_2O_2 does have this effect. The treatment of the *in vitro* BBB model with 1.0 µM H_2O_2 suggests a similar effect, in that the permeability or leakage of the BBB was increased in the presence of ROS (Figure 24, Panel B). Although preliminary, the results suggest that this model can be used to study the relationship between ROS, MMP-9 and BBB permeability.

3.6.3 Effect of conditioned media from H_2O_2-treated NRA cells on the in vitro BBB model

The previous result suggested that ROS was capable of inducing BBB leakage. I then wanted to determine if conditioned media from NRA cells treated with the same concentration of H_2O_2 could have a similar effect or an even greater effect due to the presence of potentially active MMP-9 produced or released from the cell. The initial results suggest that in fact conditioned media with H_2O_2 and presumably other factors was capable of greatly increasing the BBB permeability. To determine if this permeability was due a presence of active MMP-9 in the conditioned media, MMP-9 inhibitor SB 3CT was added to the media, which demonstrated an ability of reducing BBB leakage (Figure 24, Panel C).

3.6.4 Effect of active MMP-9 recombinant and MMP-9 inhibitor on the permeability of the in vitro BBB model.

I theorized that ROS was capable of increasing BBB permeability by activating latent forms of MMP-9 and increasing MMP-9 expression. This led me to test whether active MMP-9 could have a similar effect on BBB permeability. The result indicates a small increase in permeability in the presence of active MMP-9 and that the addition of MMP-9 inhibitor SB-3CT was able to reduce this effect (Figure 24, Panel D).

A)

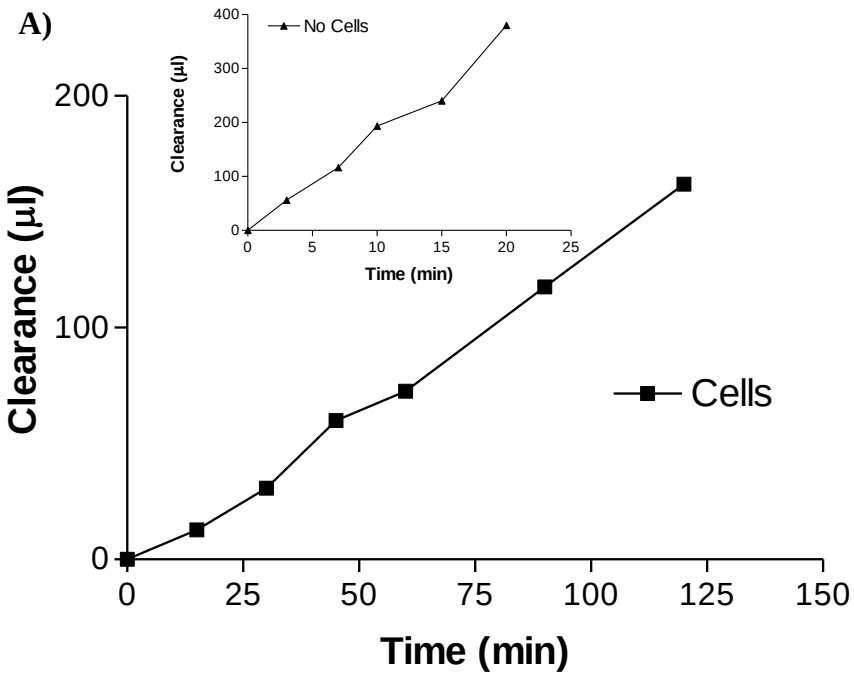
No Cells
Clearance (µl)
Time (min)
Cells
Clearance (µl)
Time (min)

B)

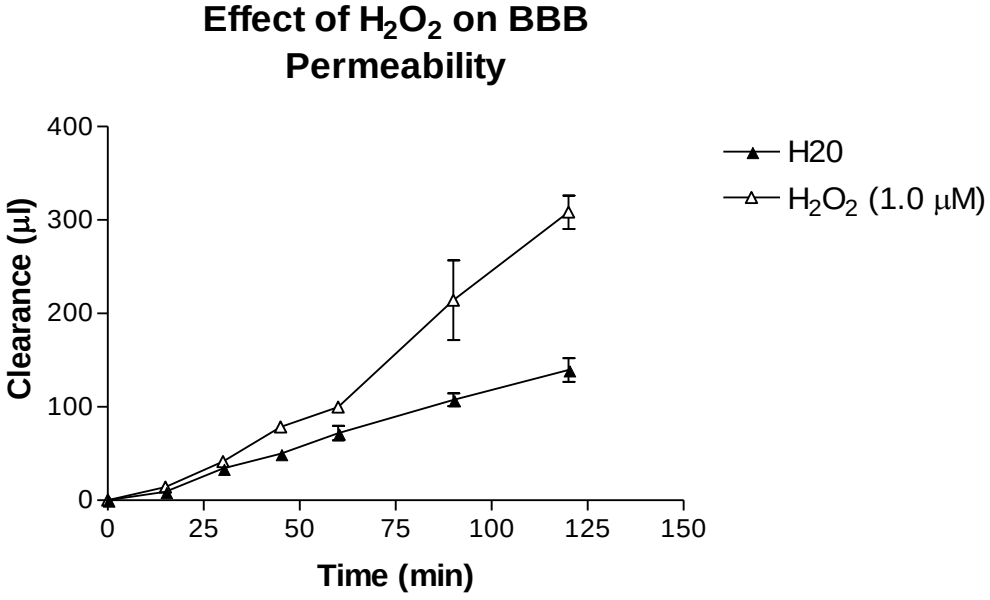
Effect of H_2O_2 on BBB Permeability
H20
H_2O_2 (1.0 µM)
Clearance (µl)
Time (min)

C)

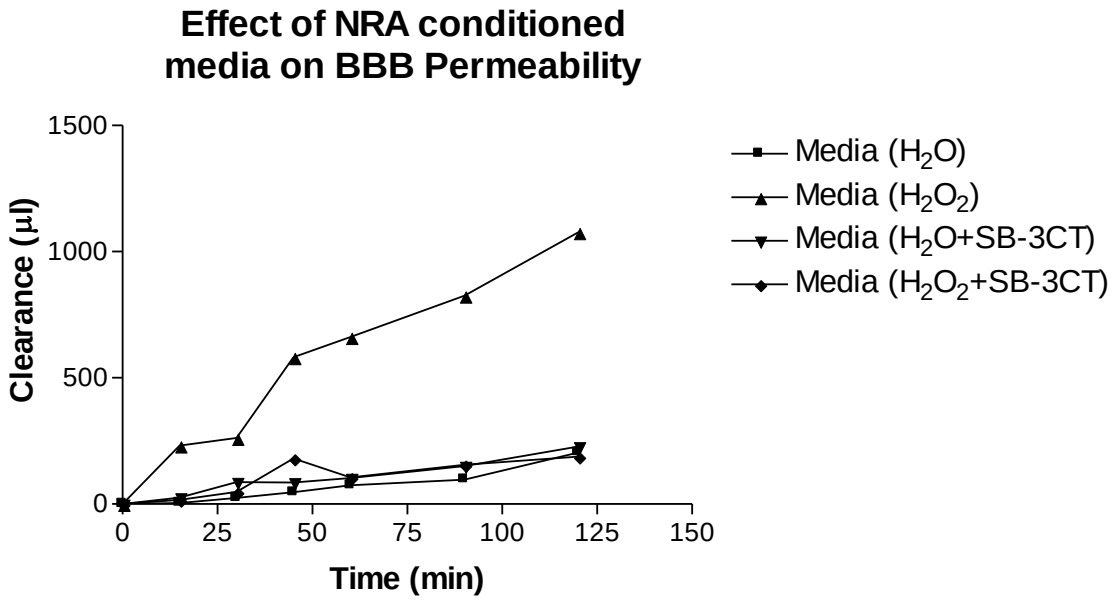
Effect of NRA conditioned media on BBB Permeability
Clearance (µl)
1500
1000
500
0
0
25
50
75
100
125
150
Time (min)
Media (H_2O)
Media (H_2O_2)
Media (H_2O+SB-3CT)
Media (H_2O_2+SB-3CT)

D)

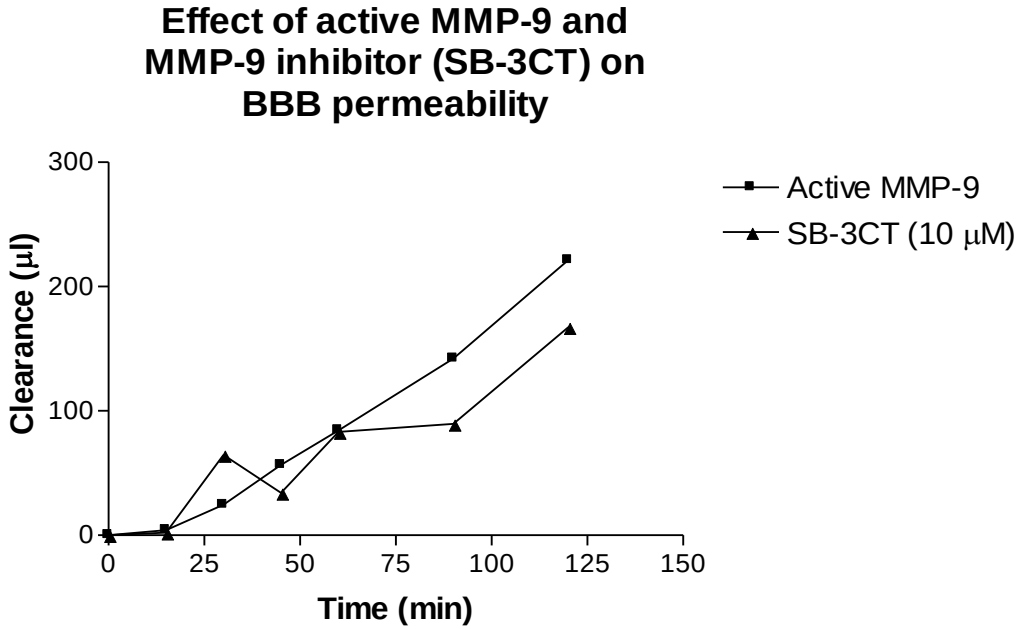
Effect of active MMP-9 and MMP-9 inhibitor (SB-3CT) on BBB permeability
Clearance (µl)
300
200
100
0
0
25
50
75
100
125
150
Time (min)
Active MMP-9
SB-3CT (10 µM)

Figure 24: Effect of H_2O_2 and MMP-9 expression on the transport of fluorescein across an *in vitro* BBB model.

The *in vitro* BBB model consists of SV-ARBEC cells grown as a monolayer on a porous membrane in the tissue culture insert. Media conditioned by rat astrocytes were applied to the bottom compartment to induce the BBB phenotype. Fluorescein (25 µg/mL) was added to the top compartment and concentrations were determined in the bottom compartment by fluorescence detection. Each time point represents one time point from preliminary experiments. **Panel A):** Permeability test was conducted determining the fluorescein concentration across triplicate membranes with and without cells. **Panel B):** H_2O_2 at concentration of 1.0 µM increases monolayer permeability and fluorescein transport across the membrane. **Panel C):** Conditioned media collected from NRA cells treated with H_2O_2 at concentration of 1.0 µM increased monolayer permeability and fluorescein transport across the membrane but treatment with MMP-9 inhibitor SB-3CT at 10 µM concentration maintained monolayer integrity and reduced fluorescein transport. **Panel D):** Active MMP-9 (25 units/mL) increased monolayer permeability and fluorescein transport across the membrane but treatment with MMP-9 inhibitor SB-3CT at 10 µM concentration maintained monolayer integrity and reduced fluorescein transport.

3.7 Recombinant TIMP-1 inhibits MMP-9 activity

As a side project of the MMP-9 signaling pathway, the endogenous inhibitor of MMP-9 tissue inhibitor of metalloproteinase 1 (TIMP-1) was cloned in an expression vector (with a his-tag), expressed in HEK293-EWCB cells and purified for use as a recombinant inhibitor. The fragmented TIMP-1 was compared to a commercial full length TIMP-1 in its ability to inhibit MMP-9 activity. The TIMP-1 fragment was capable of reducing the activity of MMP-9 (Figure 25) in a preliminary experiment, suggesting the potential for using TIMP-1 fragments as a therapeutic intervention for MMP-9 inhibition.

A)

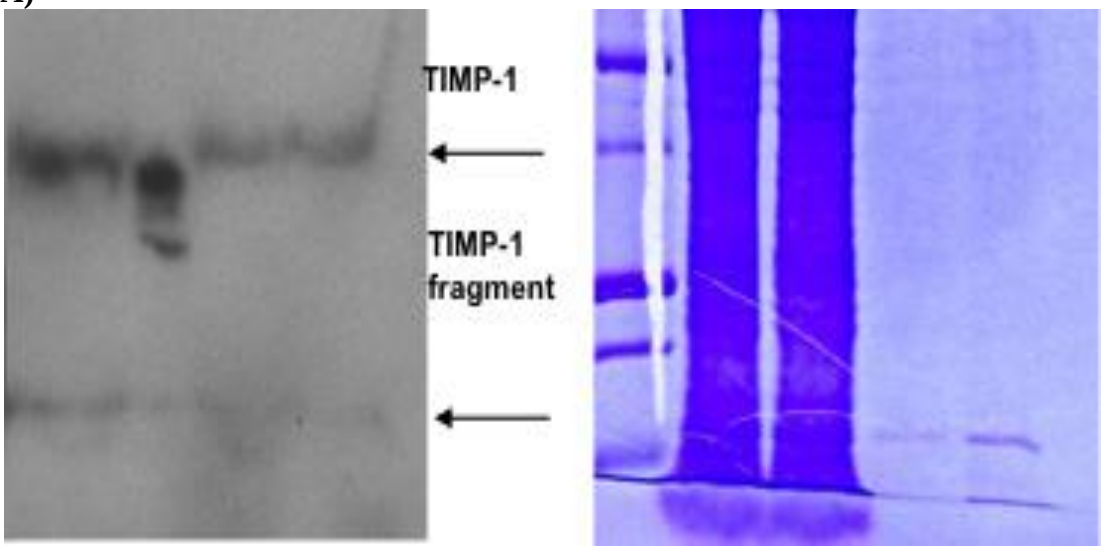

B)

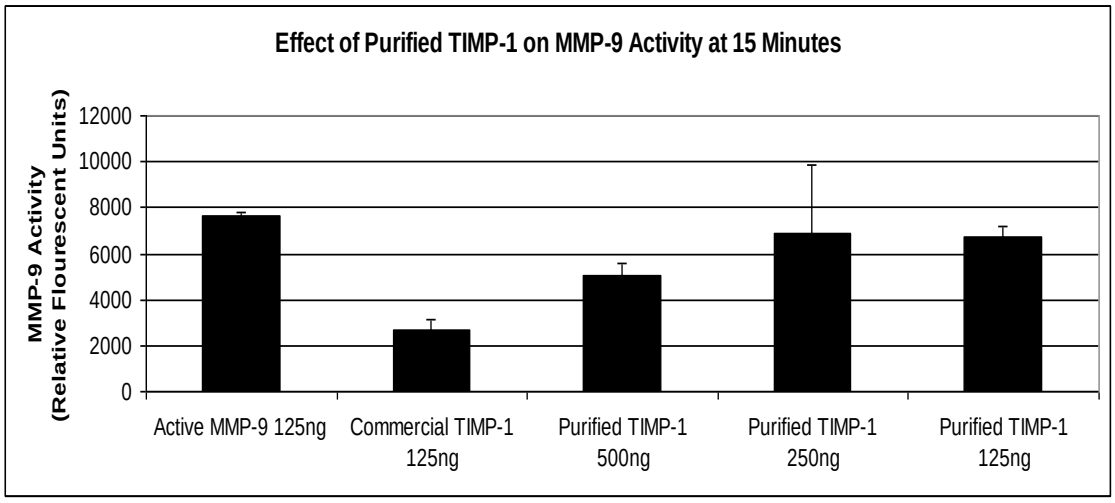

Figure 25: Cloning and purification of a recombinant TIMP-1 protein fragment for use in MMP-9 Activity Assay.

Panel A): Western blot probed with an anti-his tag antibody. TIMP-1 and a C-terminal fragment of TIMP-1 were detected in cells (C) and culture media (M). Commassie blue gel for the purification of a 15kDa C-terminal fragment from TIMP-1 protein. **Panel B)** MMP-9 activity assay to determine the inhibitory effect of recombinant TIMP-1 on MMP-9 enzyme. Commercial TIMP-1 and the purified 15kDa fragment of TIMP-1 were used in the MMP-9 activity assay. The assay shows that TIMP-1 and the TIMP-1 fragment can inhibit MMP-9 activity (N=1 data in triplicate).

Chapter 4: Discussion

MMP-9 plays a significant role in the pathology of ischemic stroke, whereby it aides in the detrimental breakdown of the blood-brain barrier; however, the signaling required for MMP-9 up-regulation has yet to be elucidated in ischemic stroke. This research is to understand whether oxidative stress affects MMP-9 expression in brain cells (astrocytes) and if so, what are the signaling pathways involved.

In this current study, I demonstrate that PMA-induced MMP-9 expression is mediated to some extent through the p38 MAP kinase signaling pathway converging on AP-1 transcription factor. In addition, I show that in a more biologically relevant model of cerebral ischemia/reperfusion, H_2O_2-induced oxidative stress stimulates a profound change in the expression of MMP-9 in a rat astrocyte cell line (NRA). This response to H_2O_2 in NRA involves activation of p38, JNK and ERK MAP kinase signaling pathways that converge onto transcription factor AP-1. In addition, a TIMP-1 fragment was used to inhibit MMP-9 activity. Furthermore, work with an *in vitro* model of the BBB suggests that active MMP-9 and H_2O_2 both increase the permeability of the BBB demonstrating their potential as therapeutic targets.

4.1 PMA stimulates MMP-9 in NRA cells via p38 kinase-AP1 signaling pathway

My research has demonstrated that treatment with PMA in astrocytes leads to MMP-9 gene expression via the p38 MAP kinase by transcription factor AP-1. This finding was supported by RT-PCR data showing an increase in MMP-9 gene expression by treatment with PMA. Furthermore, chemical inhibitors of p38 MAP kinase were able to reduce MMP-9 gene expression significantly. Lastly, reporter gene assay confirmed that transcription factor AP-1

is activated by PMA treatment. Taken together, this evidence suggests that a portion of MMP-9 gene expression in astrocytes is mediated through this pathway. My findings are supported by previous work in the field of cancer research. A human squamous cell carcinoma cell line was stimulated with PMA and was found to increase MMP-9 secretion through activation of not only p38 MAP kinase but also its downstream target MAPK2. These findings were established using a chemically specific inhibitor for p38 MAP kinase, which demonstrated a complete reduction of the PMA-induced secretion of MMP-9 (Simon *et al.* 1998). Furthermore, p38 MAP kinase was found to be signaling the PMA-induced MMP-9 activation in an AP-1 dependant manner (Simon *et al.* 2001). This finding was further supported by the work with silibinin, a flavonoid antioxidant from milk thistle that is capable of effectively blocking AP-1 via MAPK kinase signaling pathways resulting in a decrease in MMP-9 expression in MCF-7 cells (Lee *et al*. 2007). The preliminary experiments of this research were able to help establish models and positive controls for the experiments to follow but it is of interest to note, that these experiments were carried out in a brain cell culture system where the majority of work on PMA-induced MMP-9 expression via p38 MAPK signaling work has been done in carcinoma cell lines for cancer research.

4.2 H_2O_2-induced oxidative stress affects MMP-9 expression in astrocytes

My research work has shown that treating NRA cells with H_2O_2 to model the ROS generated during oxidative stress of cerebral ischemia/reperfusion results in a profound change in the expression of MMP-9. Gene expression work demonstrated that H_2O_2 induces an increase in MMP-9 expression. Interestingly, protein expression data was not as easily understood as western blot results showed that H_2O_2 decreased the amount of parent MMP-9 (pro-MMP-9) in astrocytes. It at first seems unlikely that gene expression at the mRNA level could be

increased where protein was decreased. Thus, I hypothesized that total MMP-9 was increased but my experiment was not effectively measuring total MMP-9 in astrocyte cells. In order to test this question, I used MMP activity assay to demonstrate that the amount of active MMP-9 in the conditioned media of astrocyte cells was significantly greater than controls. This suggested that in fact although the amount of MMP-9 was increased in astrocyte cells I was not able to see that with initial western blots. Finally I used immunofluorescence to determine overall amounts MMP-9 in the astrocyte cells, which further demonstrated that H_2O_2 increased MMP-9 expression in astrocytes. These findings demonstrate that in fact oxidative stress can induce MMP-9 expression at many different levels in the astrocyte cell line. These initial findings have implications for cerebral ischemia/reperfusion and ischemic stroke, whereby ROS can be identified as a key-signaling player in the activation of MMP-9 expression and the consequential BBB damage.

Stroke research in recent years has studied the effect that activated MMP-9 can have on patients and the dire neurological outcomes associated with its over-expression in early stages of stroke. However, the mechanisms of MMP-9 activation and up-regulation are not fully defined. For example, MMP inhibition has been shown to prevent the oxidative stress-associated BBB disruption following cerebral ischemia. This study suggested that oxidative stress mediates BBB disruption by activation of MMPs (Gashe *et al*. 2001). Furthermore, a link between hyperglycemia, a conditioned highly associated with cerebral ischemia, has been shown to increase oxidative stress in stroke patients. The research also found a consequential increase in MMP-9 activity and BBB breakdown, leading these authors to suggest superoxide overproduction was the fundamental link between hyperglycemia, MMP-9 and BBB breakdown (Kamada *et al.* 2007). The relationship between ROS and

MMP-9 activation has also been studied in cardiovascular research. Whereby macrophages activated during cardiovascular injury release ROS into the extracellular space that activate MMP-2 and MMP-9, which then can degrade the collagen components of the extracellular matrix resulting in negative outcomes for patients (Galis *et al.* 1995). Cardiovascular researchers characterized the mechanism of action for ROS-mediated MMP activation, showing that *in vitro* ROS can oxidize a thiol bond responsible for activating MMP-2 and MMP-9. This suggests that macrophages activated during ischemia and reperfusion that release ROS can trigger the activation of stored latent forms of MMP-9 in the vascular regions of the BBB (Rajagoplan *et al.* 1996). My work adds to this body of literature indicating that ROS produced by oxidative stress during cerebral ischemia/reperfusion can induce the expression and activate MMP-9.

4.3 ROS-induced MMP-9 expression is mediated via MAPK signaling pathways in astrocytes

Having established that in the model a relationship between ROS and MMP-9 up-regulation existed, the objective was to determine which pathways could be signaling MMP-9 expression. Previous research suggested a link between MAP kinase signaling pathways and MMP-9. Each pathway, specifically p38, JNK and ERK1/2, was studied for activation during H_2O_2 treatment to determine if they were effective by oxidative stress. Protein work demonstrated that phosphorylation levels of p38 and JNK kinase were greatly increased with ROS treatment. In contrast, phosphorylation levels of ERK 1/2 kinase was not profoundly changed. Previous research on the MAPK signaling pathways has shown that the same types of stimuli generally affect p38 and JNK kinase such as environmental stressor such as heat,

osmotic shock, and UV light, in contrast, ERK1/2 is activated by growth factors and tumor promoters (Simon et al. 2001). The phosphorylation profiles lead me to believe that the MAP kinase signaling cascades could be the upstream activators of MMP-9 gene expression, specifically p38 and JNK. Chemically specific inhibitors of MAP kinases were used to determine the effect of blocking these pathways would have on gene and protein expression. As expected, the inhibitors were able to significantly reduce the gene expression and further decrease the protein expression of MMP-9. All three inhibitors are involved, to some degree, in inhibiting the signaling of MMP-9, as no one inhibitor was capable of completely abolishing the expression, but were capable of significantly reducing it. This work also helped to clarify what was occurring with H_2O_2 treatment and MMP-9 gene expression, revealing that although the parent MMP-9 form (pro-MMP-9) was decreased, the cleaved MMP-9 (active MMP-9) was increased significantly with the treatment. Thus, H_2O_2 treatment was signaling the production of more MMP-9 protein through increased message revealed in gene expression work, but also effectively cleaving the parent protein of MMP-9 generating the active form of MMP-9 which is responsible for the proteolysis of the extracellular matrix of the BBB. Inhibitors for p38, JNK and ERK were all effective in reducing the amount of MMP-9 gene expression in astrocytes, thus reducing the amount of parent MMP-9 protein produced in astrocytes. However, the chemical inhibitors were not capable of significantly reducing the amount of cleaved MMP-9 present, which indicates that although the inhibitors can prevent H_2O_2 signaling on MMP-9 transcription, they cannot inhibit H_2O_2 ability to cleave the existent parent MMP-9 (pro-MMP-9) within the astrocyte cells. Therefore, for this finding, it is important to note that the treatment with these inhibitors reduced overall MMP-9 expression in astrocytes. This was further demonstrated

by immunocytochemistry work revealing that JNK and p38 inhibitors reduced MMP-9 expression. It is of interest to note that although ERK inhibitor was capable of reducing MMP-9 expression at the mRNA level, it did not reduce overall MMP-9 expression in astrocyte cells (immunocytochemistry data not shown) and ERK was not phosphorylated by H_2O_2 stimulation as observed for p38 and JNK. To explain this, I hypothesized that perhaps ERK 1/2 is involved in MMP-9 signaling in normal physiological processes not in response to stressors. Therefore, I reanalyzed the data to determine whether ERK 1/2 inhibitor has the same effect on baseline amounts of MMP-9 gene and protein expression. However, this reanalysis did not confirm this hypothesis, as the inhibitors did not affect baseline amounts of MMP-9 in a significant manner. The research findings on MAP kinase signaling pathway and MMP-9 expression have implications for potential therapies that aim to reduce the amount of MMP-9 in a stroke patient. For stroke patients, it is necessary to block further generation of MMP-9 but also to prevent stored latent forms of MMP-9 being activated by ROS and disturbing the permeability of the BBB.

The data generated from using chemical inhibitors for p38, JNK and ERK 1/2 highlights their potential role in the regulation of the signaling and MMP-9 expression. However, the limitations of using only chemical inhibitors must be considered as the MAPK signaling pathway is involved in a multitude of signaling processes within the cell. The conclusiveness of this finding would be ameliorated with the addition of a second methodology reducing MMP-9 through blocking the MAPK signaling pathway. For example, two different structural chemical inhibitors could have been used, one on the MAPK and one on its upstream activator MAPKK. An example of this would be for p38 signaling inhibiting not only p38 but also the MKK 3 or MKK 6, which are known

activators of p38 kinase pathway. Gene knockdown or knockout by siRNA is another alternative methodology that could bring strength to my findings.

The last aspect of characterizing the signaling pathways for MMP-9 up-regulation is the transcription factor that activates transcription of the gene of interest. The MAP kinase signaling pathways are well conserved and composed of a well-studied family of kinases known to converge on AP-1 transcription factor. Thus, previous research serves to have us start by examining a link between H_2O_2 treatment and AP-1 transcription factor. The reporter gene assays with the vectors containing the two upstream AP-1 binding sites from human MMP-9 and the classic AP-1 binding sites showed significantly greater luminescence (luciferase activity), indicating that H_2O_2 could influence MMP-9 gene expression through AP-1. To link MAP kinases to MMP-9 gene regulation, I treated the transfected cells with chemical inhibitors. These results were not as conclusive for both vectors but indicated that for the vector carrying AP-1 binding sites from MMP-9 gene, all three MAP kinases inhibitors reduced the reporter gene activity. This confirms that in fact MAP kinases can activate MMP-9 gene expression to some degree through AP-1 transcription factor. It is important to note that NFκB activation is highly associated with H_2O_2 signaling. Thus, NFκB could also play a role in both MMP-9 signaling and ROS following cerebral ischemia/reperfusion. The signaling pathway research presented is significant in demonstrating the complexity of MMP-9 up-regulation in brain cells as well as other pathologies where MMP-9 is involved such as rheumatoid arthritis and cancer. Characterization of MMP-9 is difficult due to its varying forms and the ability of molecules such as ROS to both activate latent forms of MMP-9 as well as to induce signaling for generation of MMP-9. In addition, the three MAP kinase-signaling pathways have been

shown in this research to play to some extent a role in MMP-9 signaling. This suggests that although one signaling pathway may be inhibited, there could be still generation and compensation by other pathways. Furthermore, previous research by our laboratory and others has demonstrated a role for other signaling pathways converging on NFκB transcription factor. Past research has shown that PMA induces MMP-9 via protein kinase C and via NFκB in lung epithelial cells, TNF-α stimulates MMP-9 via JNK and transactivation of NFκB (Lin *et al.* 2008), and IL-1β activates MMP-9 via ROS and NFκB transcription factor in murine macrophage cells (Yoo *et al.* 2002).

4.4 Preliminary results with the in vitro BBB model

To achieve a more conclusive representation of how my results on the MMP-9 signaling pathway could be used to prevent changes to BBB permeability in ischemic stroke, I used an *in vitro* model of the BBB. Initially, I needed to determine how H_2O_2 itself would affect the *in vitro* BBB barrier before determining how I could use the signaling pathways to down-regulate MMP-9 expression and activity. There were several caveats to this part of the study, which is the reason why I present only preliminary findings and trends with no conclusive results. The presence of H_2O_2 had an effect on the barrier, which led me to attempt removing the H_2O_2 from the media, but under these conditions I did not see a change in monolayer permeability. This finding suggests either H_2O_2 on its own was disrupting the monolayer or H_2O_2 needed to be present longer to activate MMP-9. This required the introduction of active MMP-9 to determine if MMP-9 on its own would affect BBB permeability, which in fact is appeared to do. Taken in combination, these preliminary results suggest that both H_2O_2 and MMP-9 play a role in disrupting monolayer integrity in the *in vitro* BBB model. In

addition, it seems that treatment with MMP-9 inhibitor was able to reduce the monolayer damage caused by NRA-conditioned media containing H_2O_2 and MMP-9. Although this work is preliminary, it provides the insight into what treatments may be effective in preventing MMP-9-mediated BBB breakdown in ischemic stroke. Future work will be done in our laboratory to determine what effect MMP-9, H_2O_2 and modulated MAP kinase signaling pathways could have on the *in vitro* BBB permeability.

4.5 TIMP-1 and MMP-9

The side project using a fragment of TIMP-1 protein was started to determine if the known endogenous inhibitor of MMP-9 could affect MMP-9 activity. In our preliminary experiment it seems our cleaved 15 kDa fragment is able to inhibit MMP-9 activity in a similar way as full length 28 kDa TIMP-1. The next step for this project is to sequence the TIMP-1 fragment to determine which part of the protein we have and the mechanism of inhibition.

4.6 Future Directions

This research set out to provide insight into the regulatory mechanism of MMP-9 up-regulation at the molecular level in an *in vitro* model of oxidative stress. I have demonstrated that all three MAPK signaling pathways play a role in the regulation of MMP-9 at the mRNA and protein levels with increased MMP-9 activity. My work suggests that MAPK signaling pathways be at least partially responsible for MMP-9 up-regulation induced by oxidative stress and provides the basis for testing the findings in an animal stroke model where it could reveal a more profound biological significance. Using the MCAO model for ischemic stroke, one could demonstrate that modulation of MMP-9 expression

through MAPK inhibition may affect functional/ behavioural outcomes. Therefore, targeting and modulating MMP-9 expression through the MAPK-AP1 pathway may reduce vascular and brain damage. The findings of this study could provide the basis for possible future therapeutic intervention to reduce BBB degradation and consequent brain damage mediated by MMP-9 in ischemic stroke.

Although, I have suggested that MMP-9 be a therapeutic target for ischemic stroke patients, the dual nature of MMP-9 activity in the brain must be considered. During initial stroke onset (hours to days) MMP-9 has detrimental effect, that have been dire neurological effects previously mentioned. However, during the late phases of cerebral ischemia, recent research has established a beneficial role for MMP-9 in neurovascular remodeling and brain repair (Cunningham 2005). The beneficial role of MMP-9 in stroke was highlighted by a recent study demonstrating an increase in MMP-9 in the peri-infarct area 7-14 day days after cerebral ischemia in rats. MMP inhibitors at 7 days were apple to suppress neurovascular remodeling, resulting in increased brain injury and decreased functional outcomes. The authors suggest the reduction of MMP-9 by the inhibitors reduces the amount of available VEGF to assist in vascular remodeling (Zhao *et al*. 2006). The possible beneficial roles of MMP-9 is an area that needs to be further investigated in order to determine what therapeutic options would be effective for stroke patients. My research has provided insight into what molecular signaling pathways lead to MMP-9 regulation in astrocytes but it is not a simple enough answer to completely eliminate this signal if the presence of MMP-9 at late time frames has a positive effect. Perhaps, future drug therapies will need to use MMP-9 modulators that can reduce MMP-9 during the detrimental period of initial stroke onset and

return MMP-9 to baseline levels or higher levels to assist in neurovascular remodeling and brain repair.

The research work that has been presented provides insight into the molecular signaling pathways leading to ROS induced MMP-9 up-regulation. It highlights the importance of future work needing to decipher which signaling pathways may be involved in activating latent forms of MMP-9 protein and those responsible for production of new MMP-9 protein. As mentioned previous, ischemic stroke needs to be an area of ongoing research as the only current therapy (t-PA) is only effective under very specific conditions and the prevalence and impact of stroke is of major importance to the Canadian healthcare system.

References

Ahmad AA, Gassmann M, Ogunshola OO: Maintaining Blood-Brain Barrier Integrity: **Pericytes Perform Better Than Astrocytes During Prolonged Oxygen Deprivation**. *Journal of Cellular Physiology* 2009, **218**: 612-622.

Andejelkovic AV, Kerkovich D, Pachter JS: **Monocyte:astrocyte interactions regulate MCP-1 expression in both cell types**. *Journal of Leukocyte Biology* 2000, **68**: 545-552.

Arai K, Lee SR, Lo EH: **Essential role of ERK Mitogen-Activated Protein Kinase in Matrix Metalloproteinase-9 Regulation in Rat Cortical Astrocytes**. *Glia* 2003, **43**: 254-264.

Argaw AT, Gurfein BT, Zhang Y, Zameer A, John GR: **VEGF-mediated disruption of endothelial CLN-5 promotes blood-brain barrier breakdown**. *Proceedings of the National Academy of Sciences* 2008, **106**: 1977-1982.

Asahi M, Wang X, Mori T, Sumii T, Jung JC, Moskowitz MA, Fini ME, Lo EH : **Effects of matrix metalloproteinase-9 gene knock-out on the proteolysis of blood-brain barrier and white matter components after cerebral ischemia.** *Journal of Neuroscience* 2001, **19**: 7724-7732.

Bates DO, Hillman, NJ, Williams B, Neal CR, Pocock TM: **Regulation of microvascular permeability by vascular endothelial growth factors**. *Journal of Anatomy* 2002, **200**: 581-597.

Bodden MK, Harber GJ, Birkedal-Hansen B, Windsor LJ, Caterina NCM, Engler JA, Birkedal- Hansen H: **Functional Domains of Human TIMP-1 (Tissue Inhibitor of Metalloproteinases)**. *The Journal of Biochemistry* 1994, **269**: 18943-18952.

Boulous S, Meloni BP, Arthur PG, Majda B, Bojarski C, Knuckey NW**: Evidence that intracellular cyclophilin A and cyclophilin A/CD147 receptor mediated ERK1/2 signaling can protect neurons against in vitro oxidative and ischemia injury**. *Neurobiology of Disease* 2007, **25**: 54-64.

Chen Y, Hallenbeck JM, Ruetzler C, Bol D, Thomas K, Berman NE, Vogel SN: **Overexpression of monocyte-chemoattractant protein-1 in the brain exacerbates ischemic brain injury and is associated with recruitment of inflammatory cells.** *Journal of Cerebral Blood Flow and Metabolism* 2003, **23**:748-755.

Cunningham L, Wetzel M, Rosenberg GA: **Multiple roles for MMPs and TIMPs in cerebral ischemia**. *Glia* 2005, **50**: 329-339.

Cross AK, Woodroofe MN: Chemokine **Modulation of Matrix Metalloproteinase and TIMP Production in Adult Rat Brain Microglia and a Human Microglial Cell Line in Vitro**. *Glia* 1999, **28**: 183-189.

Dai WJ, Funk A, Herdegen T, Unger T, Culman J: **Blockade of Central Angiotensin AT1 receptors improves neurological outcome and reduces expression of AP-1 trancription factors after focal brain ischemia in rats**. *Stroke* 1999, **30**: 2391-2399.

Fager N, Jaworski DM: **Differential spatial distribution and temporal regulation of tissue inhibitor of metalloproteinase mRNA expression during rat central nervous system development**. *Mechanisms of Development* 2000, **98**: 105-109.

Farkas E, Luiten PGM: **Cerebral microvascular pathology in aging and Alzheimer's disease**. *Progress in Neurobiology* 2001, **64**: 575-611.

Fenstermacher J, Gross P, Sposito N, Acuff V, Pettersen S, Gruber K: **Structural and Functional Variations in Capillary Systems within the Brain**. *Annals of the New York Academy of Sciences* 1988, **529**: 21-30.

Fujimura M, Gasche Y, Fujimura-Morita Y, Massengale J, Kawase M, Chan PK: **Early appearance of activated matrix metalloproteinase-9 and blood brain barrier disruption in mice after focal cerebral ischemia and reperfusion**. *Brain Research* 1999, **842**: 92-100.

Gabhann M, Popel AS: **Systems biology of vascular endothelial growth factors**. *Microcirculation* 2008, **8**: 715-738.

Galis ZS, Sukhova GK, Libby P: **Microscopic localization of active proteases by in situ zymography: detection of matrix metalloproteinase activity in vascular tissue**. *Federation of American Societies for Experimental Biology 1995,* **10**:974–980.

Gardner J, Ghorape A: **Tissue Inhibitor of Metalloproteinase (TIMP)-1: The TIMPed Balance of Matrix Metalloproteinases in the Central Nervous System**. *Journal of Neuroscience Research* 2003, **74**: 01-806.

Gasche Y, Copin JC, Sugawara T, Fujimura M, Chan PK: **Matrix metalloproteinase inhibition prevents oxidative stress-associated blood-brain-barrier disruption after transient focal cerebral ischemia**. *Journal of Cerebral Blood Flow and Metabolism* 2001, **21**: 1393-1400.

Genersch E, Haye K, Neuenfeld Y, Haller H: **Sustained ERK phosphorylation is necessary but not sufficient for MMP-9 regulation in endothelial cells: involvement of Ras-dependant and independent pathways**. *The Journal of Cell Science* 2000, **113**: 4319-4330.

Gomez DE, Alonso DF, Yoshiji H, Thorgeirsson UP: **Tissue inhibitors of metalloproteinases: structure, regulation and biological functions**. *European Journal of Cell Biology* 1997, **74**: 111-122.

Gu Z, Cui J, Brown S, Fridman R, Mobashery S, Strongin AY, Lipto SA: **A highly specific inhibitor of matrix metalloproteinase-9 rescues laminin from proteolysis and neurons from apoptosis in transient focal cerebral ischemia.** *The Journal of Neuroscience* 2005, **25**: 6401-6408.

Hamann GF, Okada Y, Fitridge R, Zoppo G.J: **Microvascular basal lamina antigens disappear during cerebral ischemia and reperfusion**. *Stroke* 1995, **26**: 2120-2126.

Harper E, Block KJ, Gross J: **Zymogen of tadpole collagenase**. *Biochemistry* 1971, **10**: 3035-3041.

Hawkins BT, Davis TP: **The Blood-Brain Barrier/ Neurovascular Unit in Health and Disease**. *Pharmacology Reviews* 2005, **57**: 173-185.

Hong S, Park KK, Magae J, Ando K, Leell TS, Kwon TK: **Ascochlorin Inhibits Matrix Metalloproteinase-9 Expression by Suppressing Activator Protein-1-mediated Gene Expression through the ERK1/2 Signaling Pathway**. *Journal of Biological Chemistry* 2005, **26**: 25202-25209.

Iwai S, Alhada A, Hida A: **Activation of AP-1 and Increase Synthesis of MMP-9 in the Rabbit Retina induced by Lipid Hydroperoxide**. *Current Eye Research* 2006, **31**: 337-346.

Iwai S and colleagues: **Activation of AP-1 and Increased Synthesis of MMP-9 in the Rabbit Retina Induced by Lipid Hydroperoxide**. *Current Eye Research* 2006, **31**: 337-346.

Junttila MR, Li SP, Westermarck: **Phosphatase-mediated crosstalk between MAPK signaling pathways in the regulation of cell survival**. *The FASEB journal* 2008, **22**: 954-965.

Kamada H, Yu F, Nito C, Chan PH: **Influence of Hyperglycemia on Oxidative Stress and Matrix Metalloproteinase-9 Activation After Focal Cerebral Ischemia/Reperfusion in Rats**. *Stroke* 2007, **38**: 1044-1049.

Kelly PJ, Morrow JD, Ning MM, Koroshetz W, Lo EH, Terry E, Milne GL, Hubbard J, Lee H, Stevenson E, Lederer M, Furie KL: **Oxidative Stress and Matrix Metalloproteinase-9 in Acute Ischemic Stroke.** *Stroke* 2008 **39**: 100-104.

Kolch W: **Coordinating ERK/MAPK signaling through scaffolds and inhibitors**. *Nature Reviews Molecular Cell Biology* 2005, **6**: 827-837.

Kniesel U, Wolburg H: **Tight Junction of the Blood-Brain Barrier**. *Cellular and Molecular Neurobiology* 2000, **20**: 59-76.

Kondo T, Reaume AG, Huang TT, Carlson E, Murakami K, Chen SF, Hoffman EK, Scott RW, Epstein CJ, Chan PH: **Reduction of CuZn-superoxide dismutase activity exacerbates neuronal cell injury and edema formation after transient focal cerebral ischemia**. *Journal of Neuroscience* 1997, **17**: 4180-4189.

Lee SR, Kim HY, Rogowska J, Zhao BQ, Bhide P, Parent JM, Lo EH: **Involvement of matrix metalloproteinase in neuroblast cell migration from the subventricular zone after stroke.** *The Journal of Neuroscience* 2006, **13**: 3491-3495.

Lee SR, Guo SZ, Scannevin RH, Magliaro BC, Rhodes KJ, Wang X, Lo EH: **Induction of matrix metalloproteinase, cytokines and chemokines in rat cortical astrocytes exposed to plasminogen activators**. *Neuroscience Letters* 2007, **417**: 1-5.

Manning A, Davis R: **Targeting JNK for therapeutic benefit: from junk to gold?** *Nature Reviews Drug Discovery* 2003, **2**: 554-565

Mojsilovic-Petrovic J, Callaghan D, Cui H, Dean C, Stanimirovic DB, Zhang W: **Hypoxia-inducible factor-1 (HIF-1) is involved in regulation of hypoxia-stimulated expression of monocyte chemoattractant protein-1 (MCP-1/CCL2) and MCP-5 (Ccl12) in astrocytes**. *Journal of Neuroinflammation* 2007, **4**: 12-27.

Montaner J, Avarez-Sabin J, Molina C, Angeles A, Abilleira S, Arenillas J, Gonazalex MA, Monasterio J: **Matrix metalloproteinase expression after human cardioembolic stroke: temporal profile, and relation to neurological impairment.** *Stroke* 2005, **36**: 1415-1420.

Mori T, Xiaoying Wang, Toshiaki Aoki, Eng H. Lo. **Downregulation of Matrix Metalloproteinase-9 and Attenuation of Edema via Inhibition of ERK Mitogen Activated Protein Kinase in Traumatic Brain Injury.** *Journal of Neurotrauma* 2002, **19**: 1411-1419.

Nagase H, Meng Q, Malinovskii V, Huang W, Chung L, Bode W, Maskos K, Brew K: **Engineering of selective TIMPs**. *Annals of New York Academy of Sciences* 1999, **878**: 1-11.

Narasimhan P, Liu J, Song YS, Massengale JL, Chan PH. **VEGF Stimulates the ERK 1/2 signaling pathway and apoptosis in cerebral endothelial cells after ischemic conditions**. *Stroke* 2009, **40**:1467-1473.

Oldendorf WH, Cornford ME, Brown WJ: **The large apparent work capability of the blood-brain-barrier: a study of the mitochondrial content of capillary endothelial cells in brain and other tissues of the rat**. *Annals of Neurology* 1977, 1: 409-417.

Pardridge WM: **Molecular biology of the blood-brain barrier**. *Molecular Biotechnology* 2005, **30**: 57-70.

Pfefferkorn T, Rosenberg GA: **Closure of the Blood-Brain Carrier by Matrix metalloproteinase inhibition reduced rtPA-mediated mortality in cerebral ischemia with delayed reperfusion.** *Stroke* 2003, **34**: 2025-2030.

Rajagopalan S, Meng XP, Ramasamy S, Harrison DG, Galis ZS: **Reactive Oxygen Species Produced by Macrophage-derived Foam Cells Regulate the Activity of Vascular Matrix Metalloproteinases In Vitro Implications for Atherosclerotic Plaque Stability**. *Journal of Clinical Investigation* 1996, **98**: 2572–2579

Ram M, Sherer Y, Shoenfeld Y: **Matrix Metalloproteinase-9 and Autoimmune Diseases**. *Journal of Clinical Immunology* 2006, **26**: 299-307.

Romanic AM, White RF, Arleth AJ, Ohlstein EH, Barone FC: **Matrix metalloproteinase expression increases after cerebral focal ischemia in rats: inhibition of matrix metalloproteinase-9 reduces infarct size.** *Stroke* 1998, **5**: 1020-1030.

Romero IA, Radeqicz K, Jubin E, Michel CC, Greenwood J, Couraud PO, and Adamson P: **Changes in cytoskeletal and tight junctional proteins correlate with decreased permeability induced by dexamethasone in cultured rat brain endothelial cells**. *Neuroscience Letters* 2003, **344**: 112-116.

Rosell A, Lo EH: **Multiphasic roles of matrix metalloproteinases after stroke.** *Current Opinion in Pharmacology* 2008, **8**: 82-89.

Rosell A, Ortega-Axnar A, Alvarez-Sabin J, Fernandez-Cadenas I, Ribo M, Molina CA, Lo EH, Montaner J: **Increased brain expression of matrix metalloproteinase-9 after ischemia and hemorrhagic human stroke.** *Stroke* 2006, **37**: 1399-1406.

Savettieri G, Liegro I, Catania C, Licata L: **Neurons and ECM regulate occludin localization in brain endothelial cells**. *NeuroReport* 2000, **11**: 1081-1084.

Simon C, Goepfert H, Boyd D: **Inhibition of the p38 mitogen-activated protein kinase by SB 203580 blocks PMA-induced M_r 92,000 type IV collagenase secretion and in vitro invasion**. *Cancer Research* 1998, **58**: 1135-1139.

Simon C, Simon M, Vucelic G, Hicks MJ, Plinkert PK, Koitschev A, HP Zenner: **The p38 SAPK Pathway Regulates the Expression of the MMP-9 Collagenase via AP-1 Dependant Promoter Activation.** *Experimental Cell Research* 2001, **271**:344-355.

Shukla A, Shukla R, Dikshit M, Srimal RC. **Alterations in free radical scavenging mechanisms following blood-brain barrier disruption.** *Free Radical Biology and Medicine* 1993, **15**: 97-100.

Sternlicht MD, Werb Z: **How matrix metalloproteinases regulate cell behavior**. *Annual Reviews Cell Developmental Biology* 2001, **17**: 463-516.

Stocker W, Bode W: **Structural features of the superfamily of zinc-endopeptidases: the metzincins**. *Current Opinion in Structural Biology* 1995, **5**: 383-390.

Tagami M, Nara Y, Fujino H, Yamori Y: **Ultrastructural changes in cerebral pericytes and astrocytes of stroke- prone spontaneously hypertensive rats**. *Stroke* 1990, **21**: 1064-1071.

Tan HK, Heywood D, Ralph GS, Bienemann A, Baker AH, Uney JB: **Tissue inhibitor of metalloproteinase 1 inhibits excitotoxic cell death in neurons**. *Molecular and Cellular Neuroscience* 2003, **22**: 98-106.

Uno M, and colleagues: **Elevation of plasma oxidized LDL in acute stroke patients is associated with ischemic lesions depicted by DWI and predictive of infarct enlargement.** *Neurological Research* 2005, **27**: 94-102.

Vaillant C, Didier-Bazes M, Hutter A, Belin MF, Thomasset N: **Spatiotemporal expression patterns of metalloproteinases and their inhibitors in the postnatal developing rat cerebellum**. *The Journal of Neuroscience* 1999, **19**: 4995-5004.

Vallable S, Monatoner J, Bellail A, Berezowsi V, Brillault J, Cecchelli R, Divoux D, Mackenzie ET, Bernaudin J, Roussel S, Petit E: **VEGF-induced BBB permeabililty**

is sassociated with an MMP-9 activity increase in cerebral ischemia: both effects decreased by Ang-1. *Journal of Cerebral Blood Flow and Metabolism* 2005, **25**: 1491-1504.

Wang HH, Hsieh HL, Wu CY, Sun CC, Yang CM: **Oxidized low-density lipoprotein induces matrix metalloproteinase-9 expression via a p42/p44 and JNK-dependent AP-1 pathway in brain astrocytes.** *Glia* 2009, **1**: 24-38.

Wang X, Jung J, Asahi M, Chwang W, Russo L, Moskowitz MA, Dixon CE, Fini ME, Lo EH: **Effects of matrix metalloproteinase-9 gene knock-out on morphological and motor outcomes after traumatic brain injury**. *The Journal of Neuroscience* 2000, **18**: 7037-7042.

Weiss JM, Downie SA, Lyman WD, Berman JW: **Astrocyte-derived monocyte-chemoattractant protein-1 directs the transmigration of leukocytes across a model of the human blood-brain barrier**. *Journal of Immunology* 1998, **161**:6896-6903.

Whitmarsh AJ, Davis RJ: **Transcription factor AP-1 regulation by mitogen-activated protein kinase signal transduction pathways**. *Journal of Molecular Medicine* 1996, **74**: 589-607.

Wolburg H, Lippoldt A: **Tight junctions of the blood–brain barrier: development, composition and regulation**. *Vascular Pharmacology* 2002, **38**: 323-337.

Zlokovic BV: **Remodeling after stroke.** *Nature Medicine* 2006, **12**: 390-391.

Zlokovic BV: **The Blood-Brain Barrier in Health and Chronic Neurodegenerative Disorders**. *Neuron Review* 2008, **57**: 178-199.

Zhang W, Stanimirovic D: **Current and future therapeutic strategies to target inflammation in stroke**. *Current Drug Targets Inflammation and Allergy* 2002, **2**: 151-166.

Zhang W, Stanimirovic DB. 2005: The transport systems of the blood-brain barrier. In. ***The Blood-Brain Barrier and its Microenvironment: Basic Physiology to Neurological Disease***,. pp. 103-142, Eds. De Vries E., and Prat, A., Taylor & Francis Group, New York.